Correlation between electronic structure, magnetism and physical properties of Fe-Cr alloys: ab initio modeling

Igor A. Abrikosov

Department of Physics, Chemistry, and Biology (IFM),

Linköping University, Sweden

Fe-Cr alloys

- Are the base for many important industrial steels
- Used as cladding material in fast neutron reactors
- Low Cr steels, up to 10 % Cr, show:
  anomalous stability
  resistance to neutron
  radiation induced swelling
  corrosion resistance
  increased ductile to brittle
  transition temperature

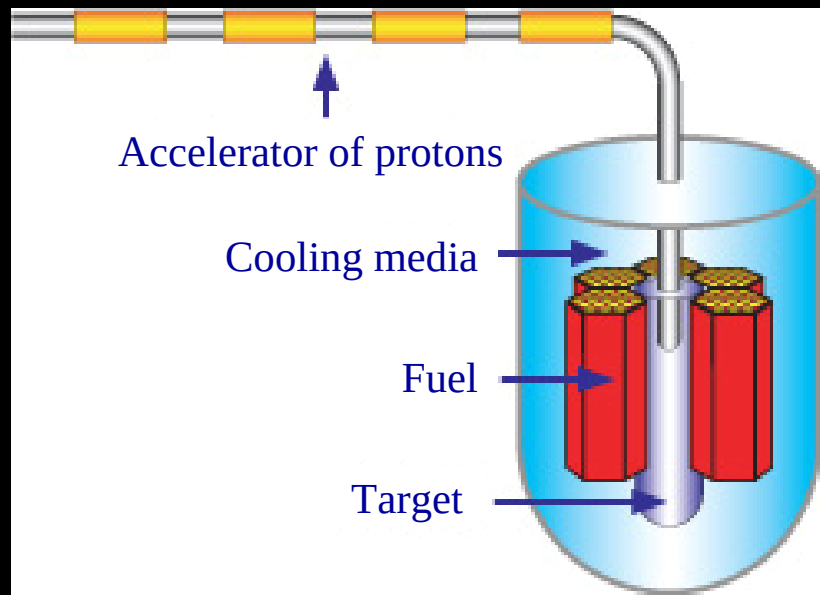

In collaboration with:

P. Olsson, EDF R&D, France

A. V. Ponomareva, MIS&A, Russia

A. V. Ruban, KTH, Sweden

L. Vitos, KTH, Sweden

J. Wallenius, KTH, Sweden

CONTENTS :

- Phase equilibria in solid solutions: theoretical background
- First-principles methods: recent developments
- Fe-Cr alloys: first-principles results
- Discussion: understanding of first-principles results
- Conclusions

Microstructure – Property Relationships

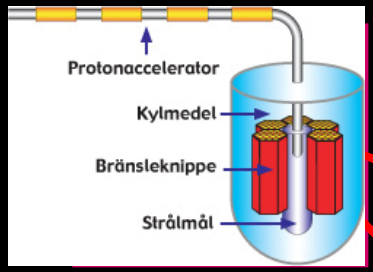

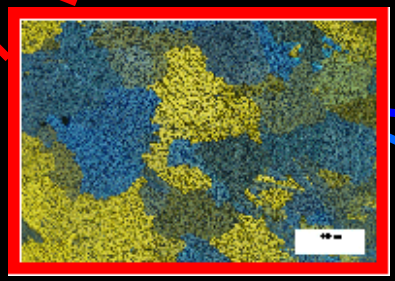

Microstructure
- Grains
≅ 1 – 10 mm
Properties
• High cycle fatigue
• Ductility

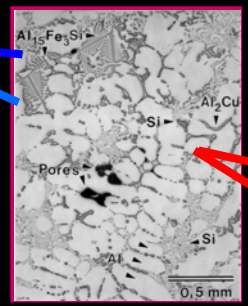

Microstructure
- Phases
≅ 100 – 500 microns
Properties
• Yield strength
• Ultimate tensile strength
• High cycle fatigue
• Low cycle fatigue
• **Thermal Growth**
• Ductility

Microstructure
- Phases
≅ 3-100 nanometers
Properties
• Yield strength
• Ultimate tensile strength
• Low cycle fatigue
• Ductility

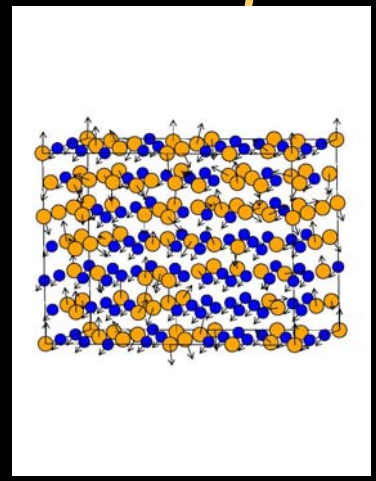

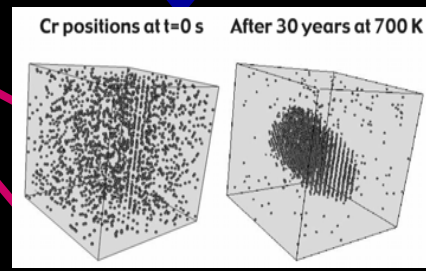

Atoms
≅ 10-100 Angstroms
Properties
• Thermal Growth

Original idea for this figure belongs to Chris Wolverton Ford Motor Company

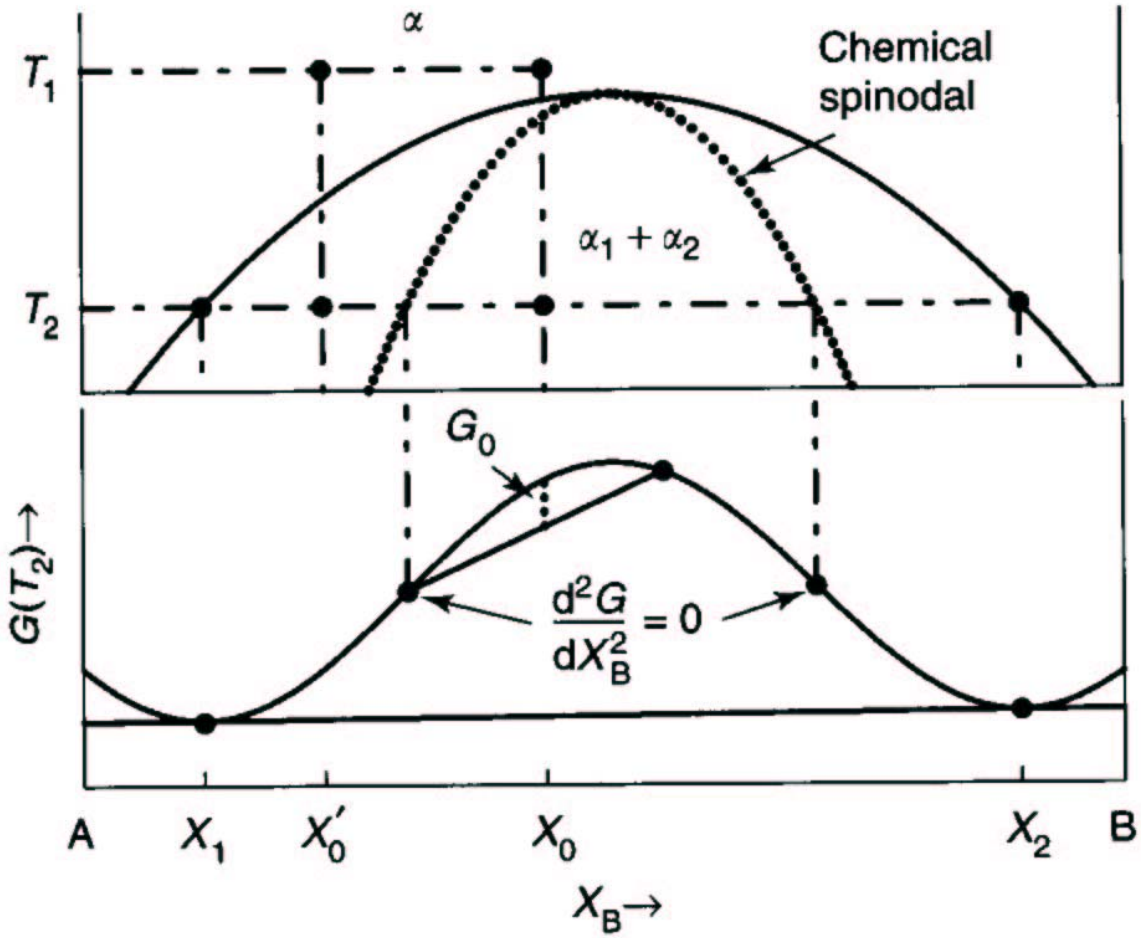

Figure 9 (a) Schematic phase diagram and (b) free energy vs. composition diagram for alloys between the spinodal points, which are unstable and can decompose into two coherent phases α_1 and α_2 without overcoming an activation energy barrier. Alloys between the miscibility gap and the spinodal are metastable and can decompose only after nucleation of the other phase.

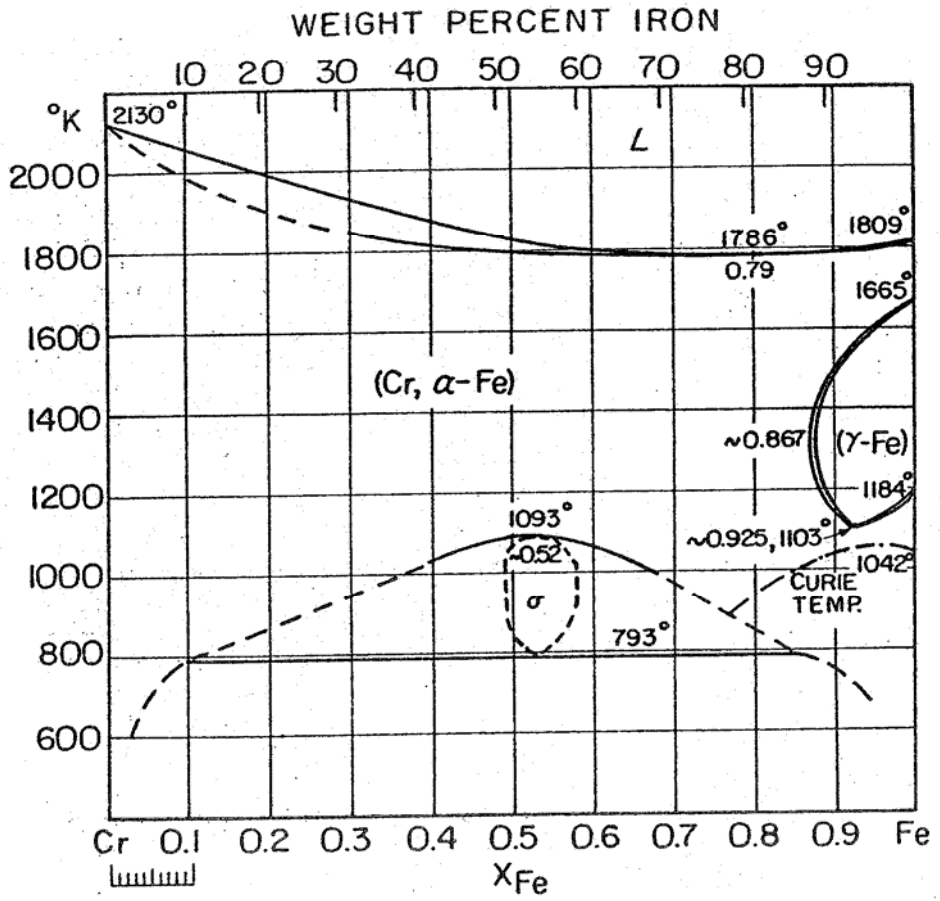

CHROMIUM-IRON SYSTEM, 1600 °K

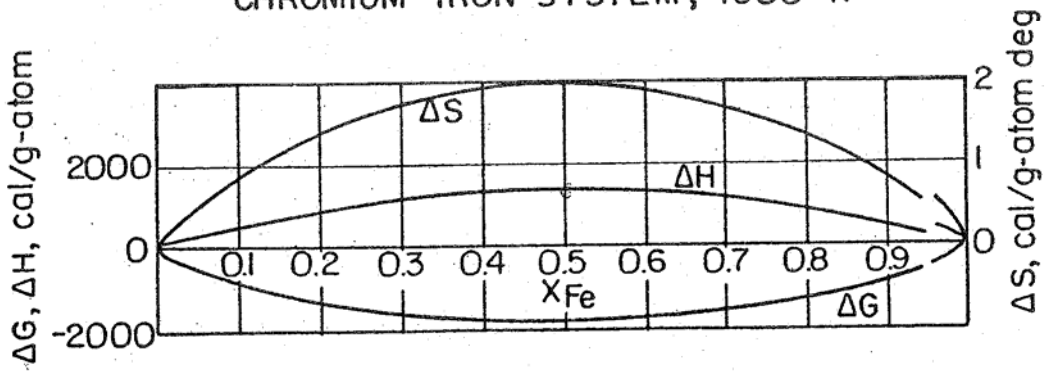

First–principles calculations

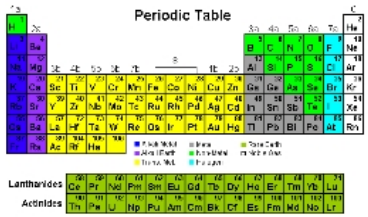

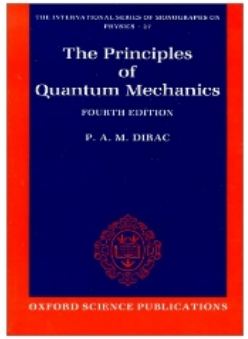

Approximations:
LDA, CPA ...
Methods:
LMTO, MD,
Monte Carlo ...

Experimental data

Adjustable parameters

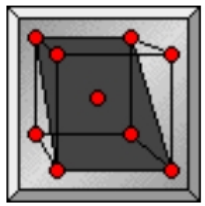

Structure

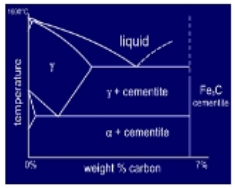

Phase equlilbria

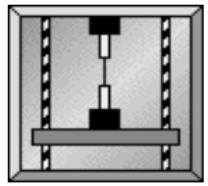

Mechanical properties

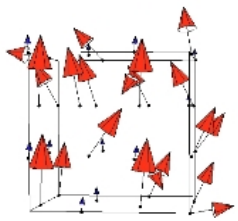

Magnetism

Fundamental understanding

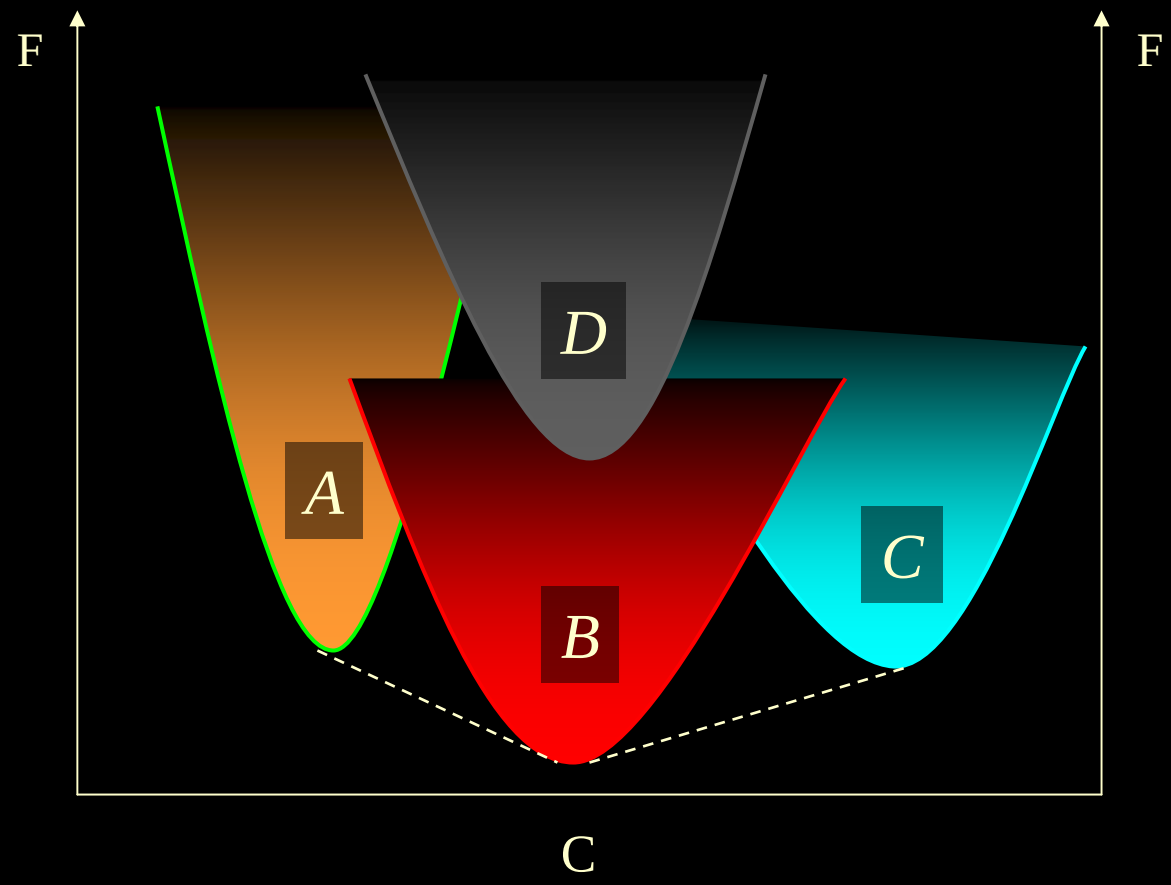

Structures:

A

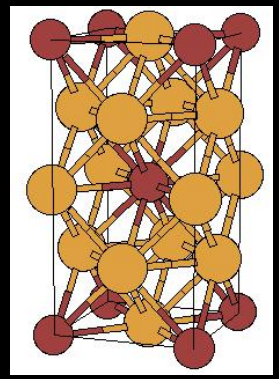

B

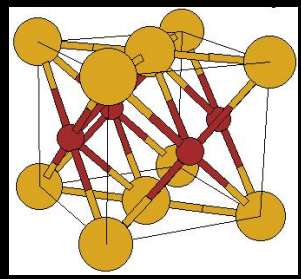

D

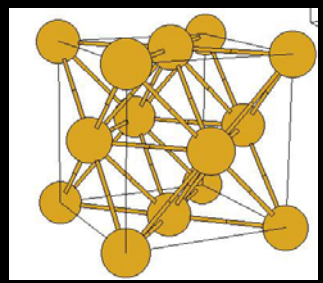

C

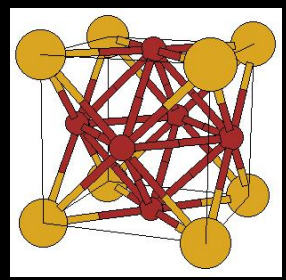

$$F = -k_B T \ln Z \qquad Z = \sum_s \exp\left(-\frac{E_s}{kT}\right)$$

A atom

B atom

A_xB_{1-x} alloy

$n(\mathbf{r})$, the electron density

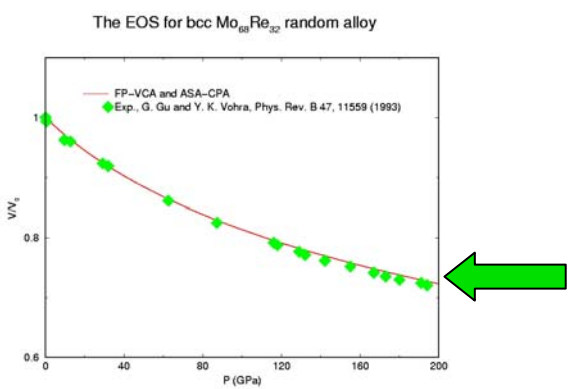

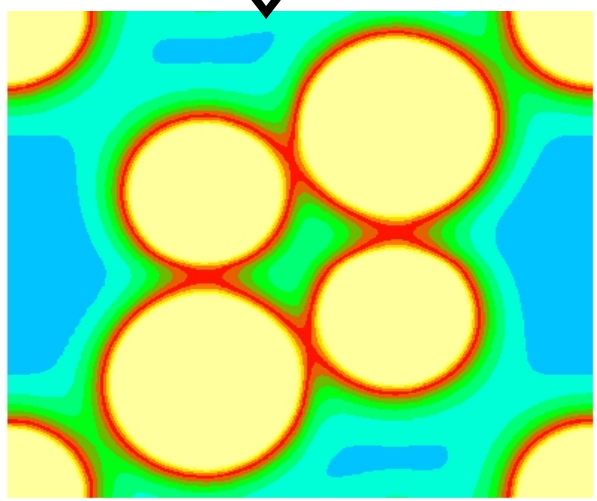

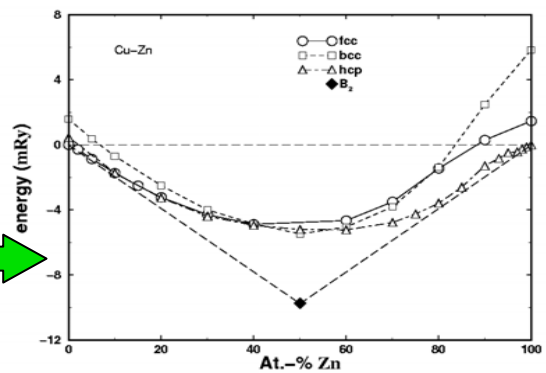

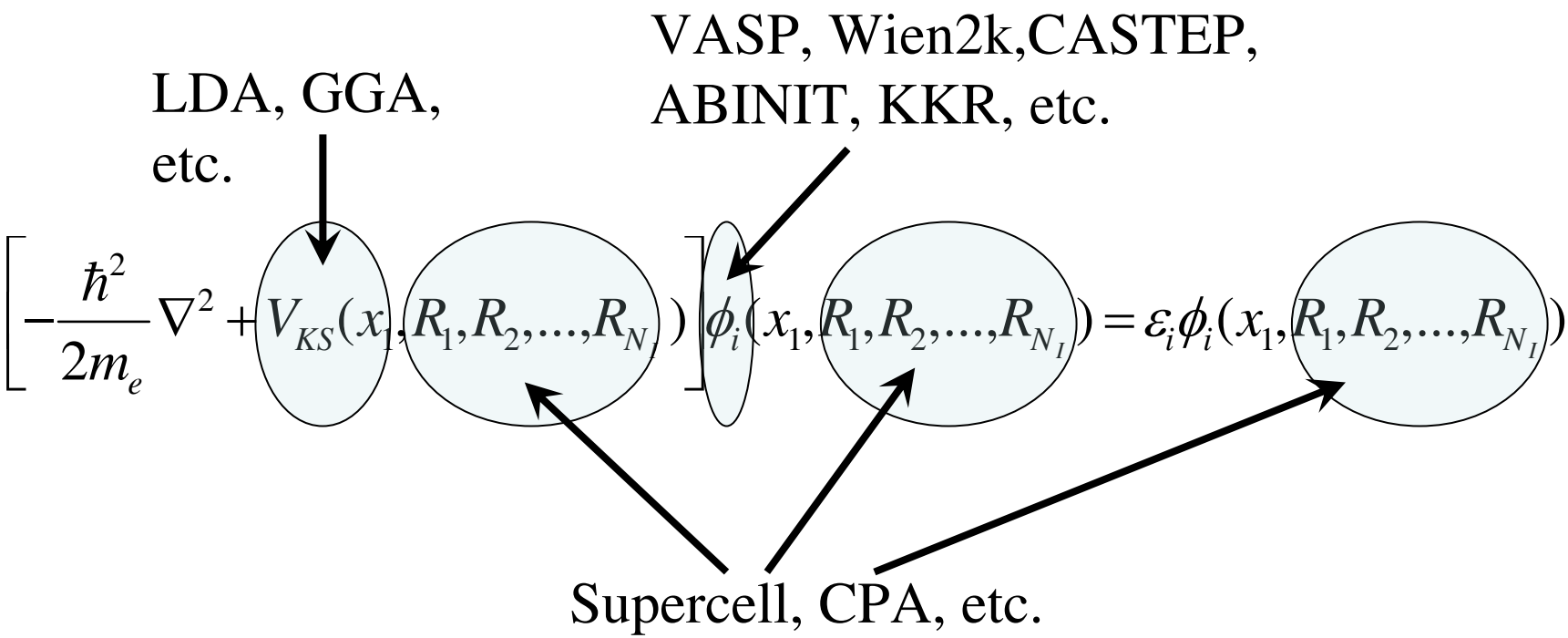

It is NOT a trivial task to run *ab initio* software!

Ordered compounds

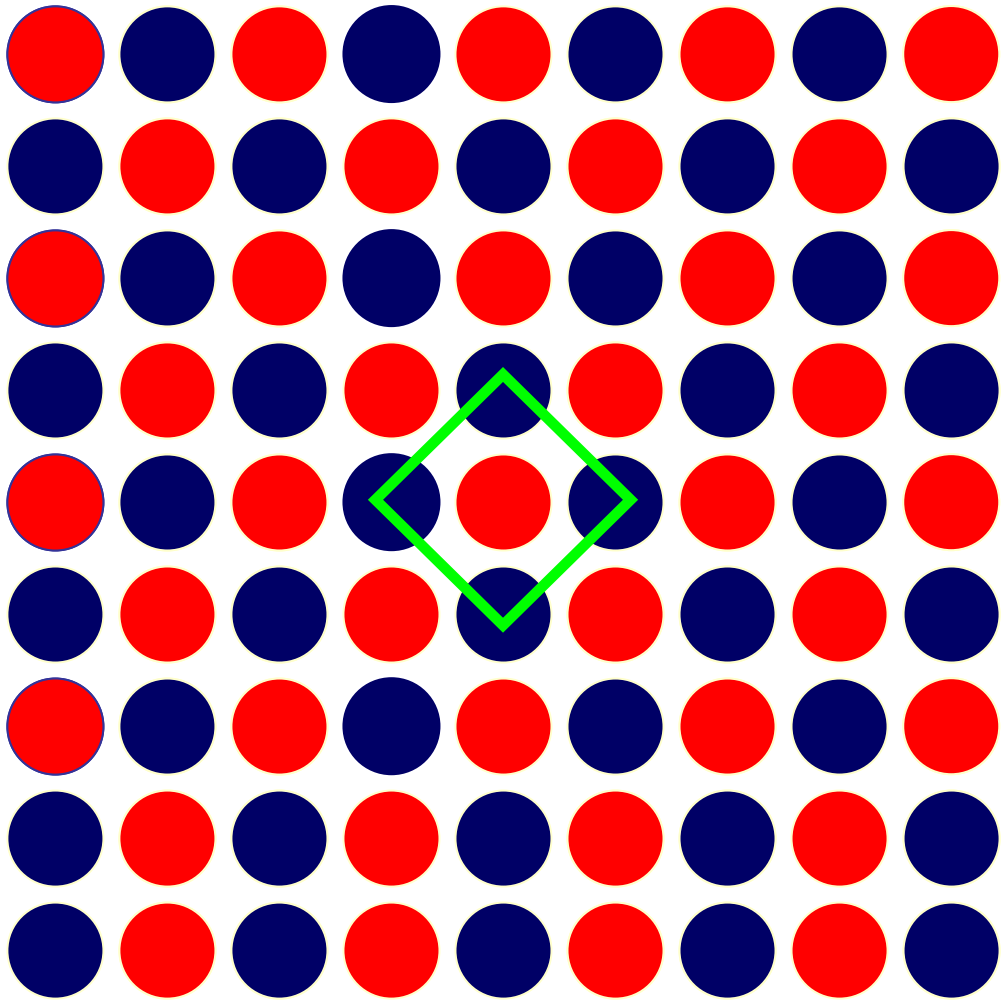

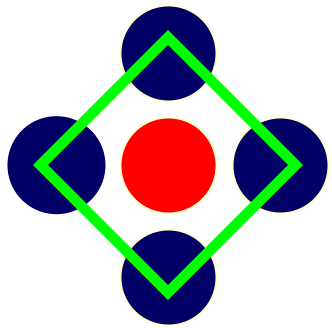

Solution phases: supercell method

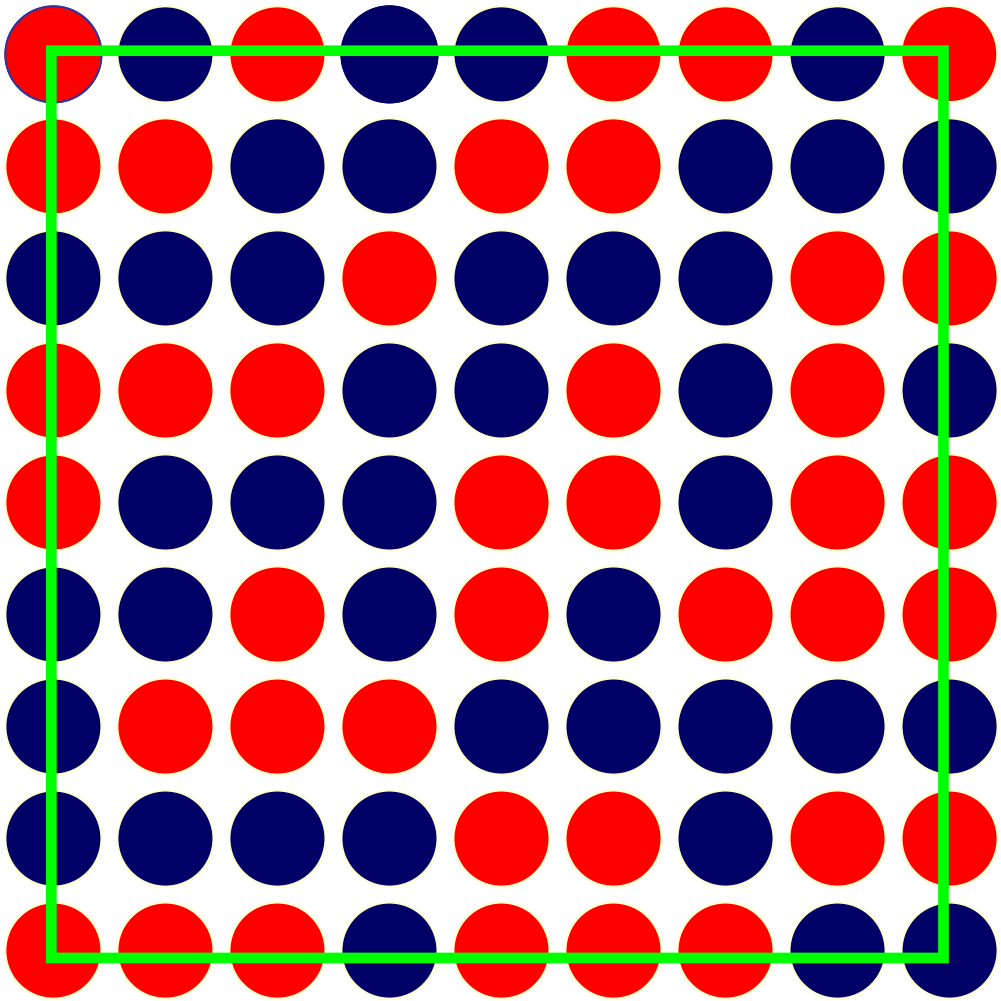

2X2X7, segregation energy -0.043 eV

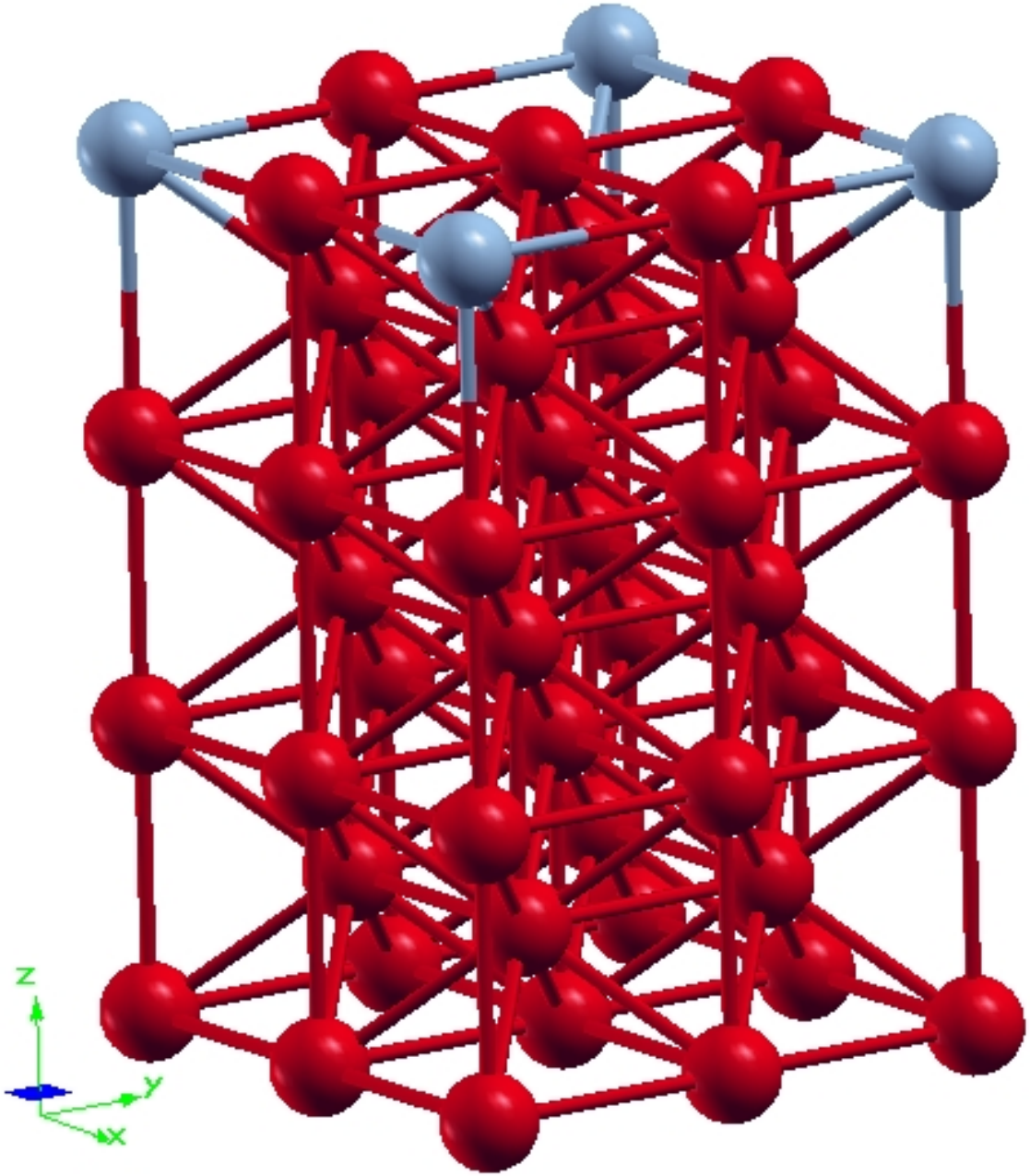

A. V. Ponomareva *et al.*, Phys. Rev. B 75, 245406 (2007)

3X3X9, segregation energy 0.090 eV

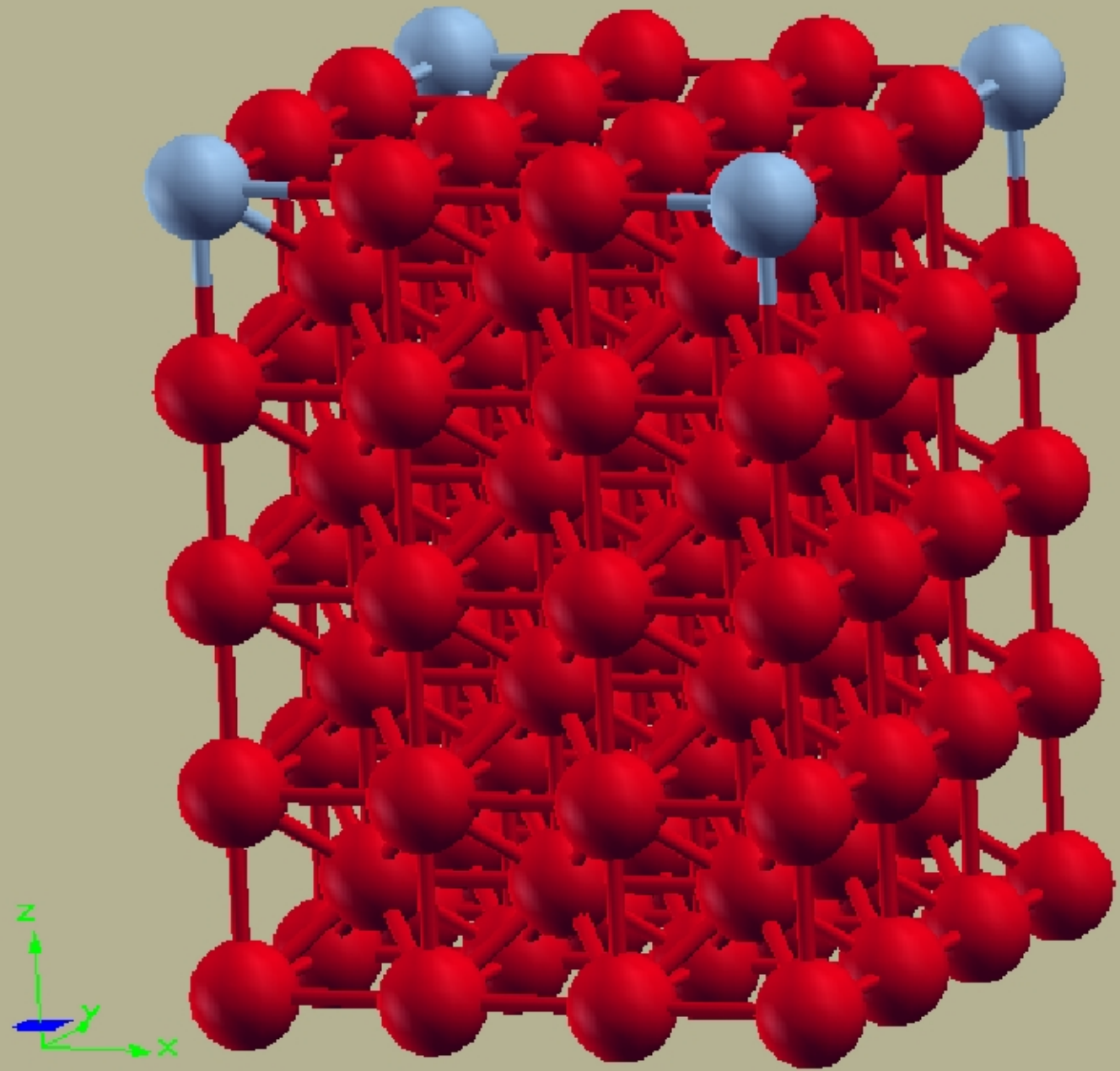

A. V. Ponomareva *et al.*, Phys. Rev. B 75, 245406 (2007)

Solution phases: coherent potential

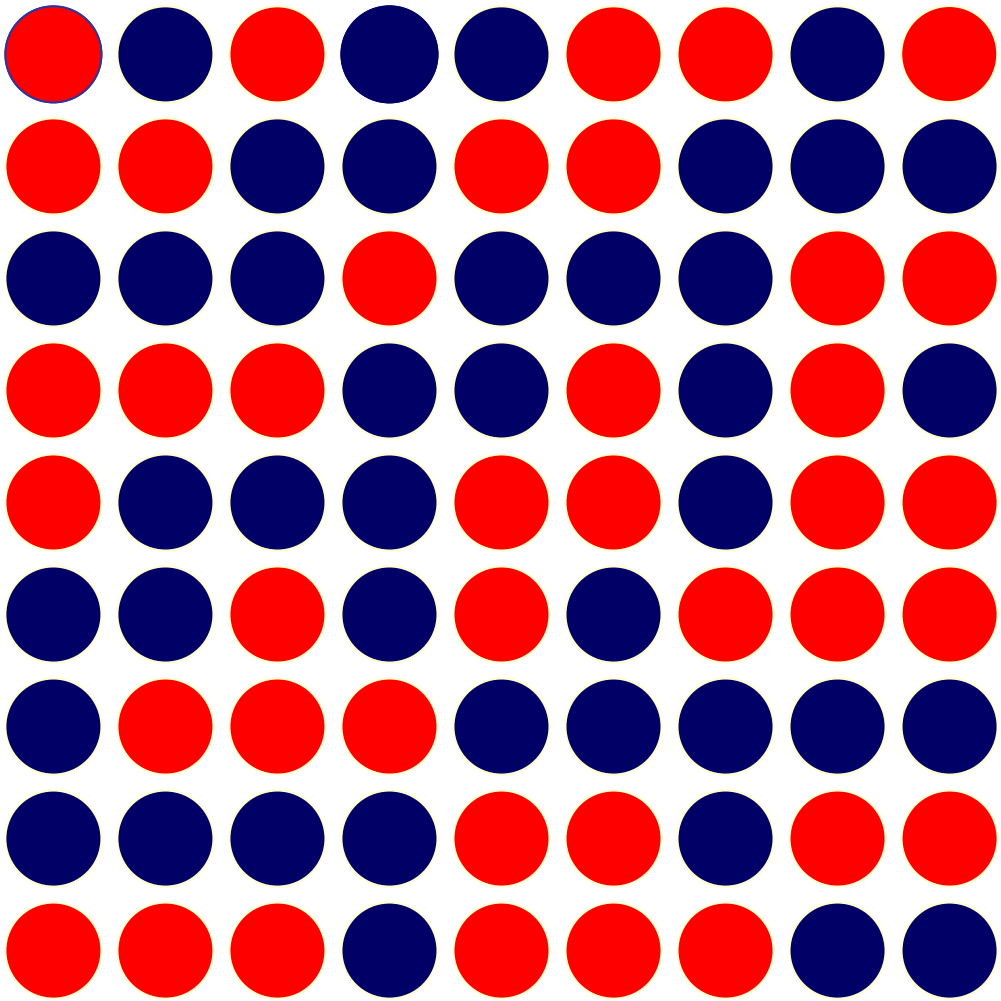

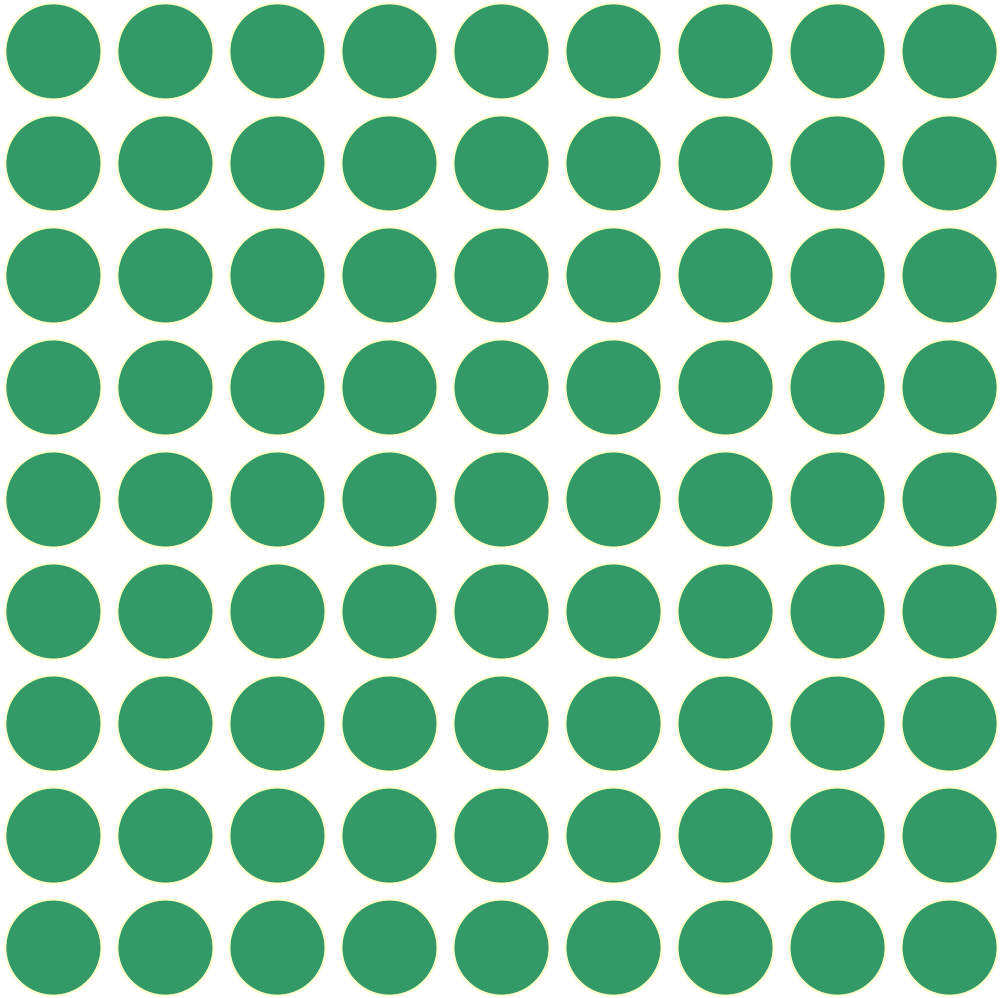

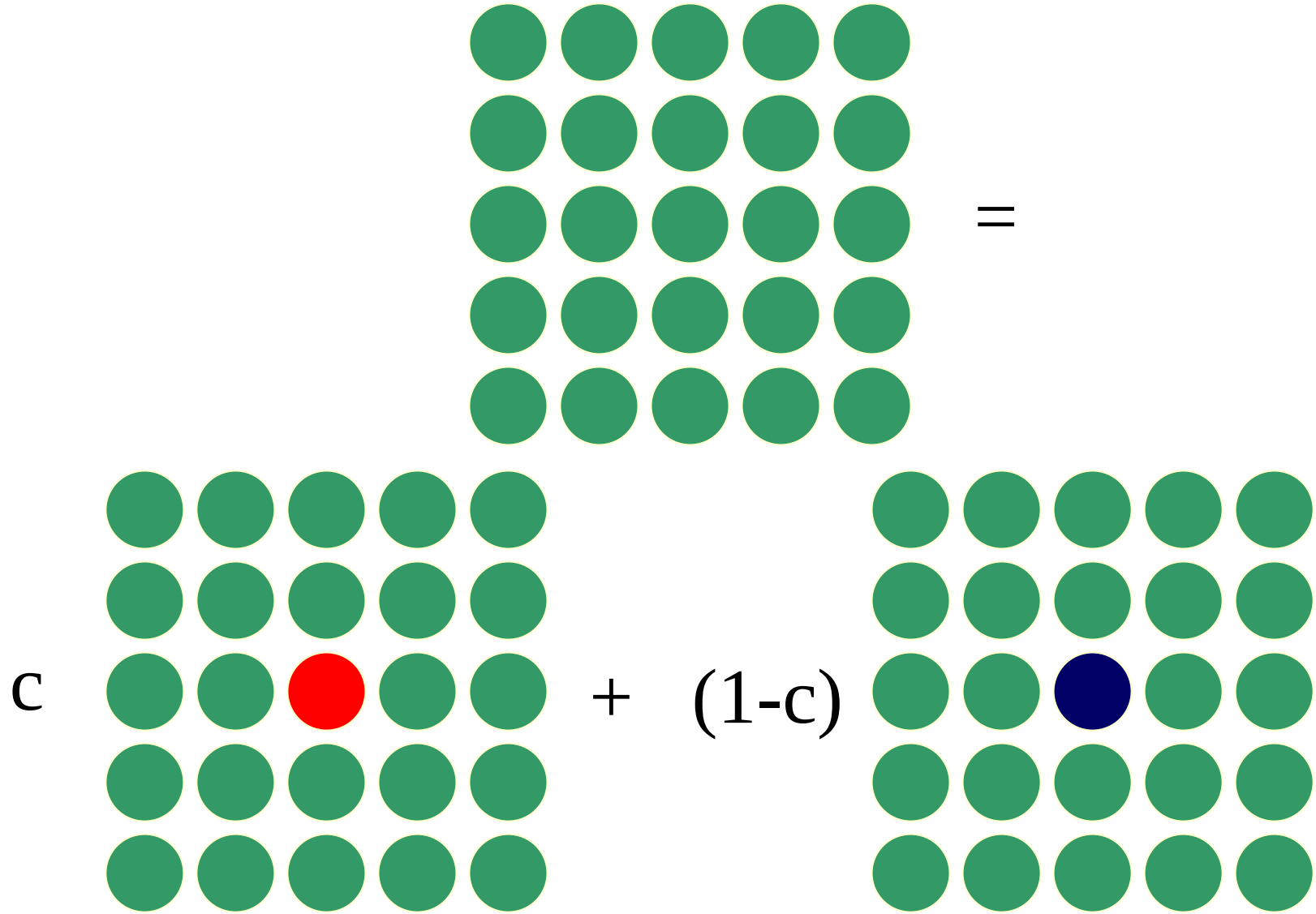
=
c
+
(1-c)

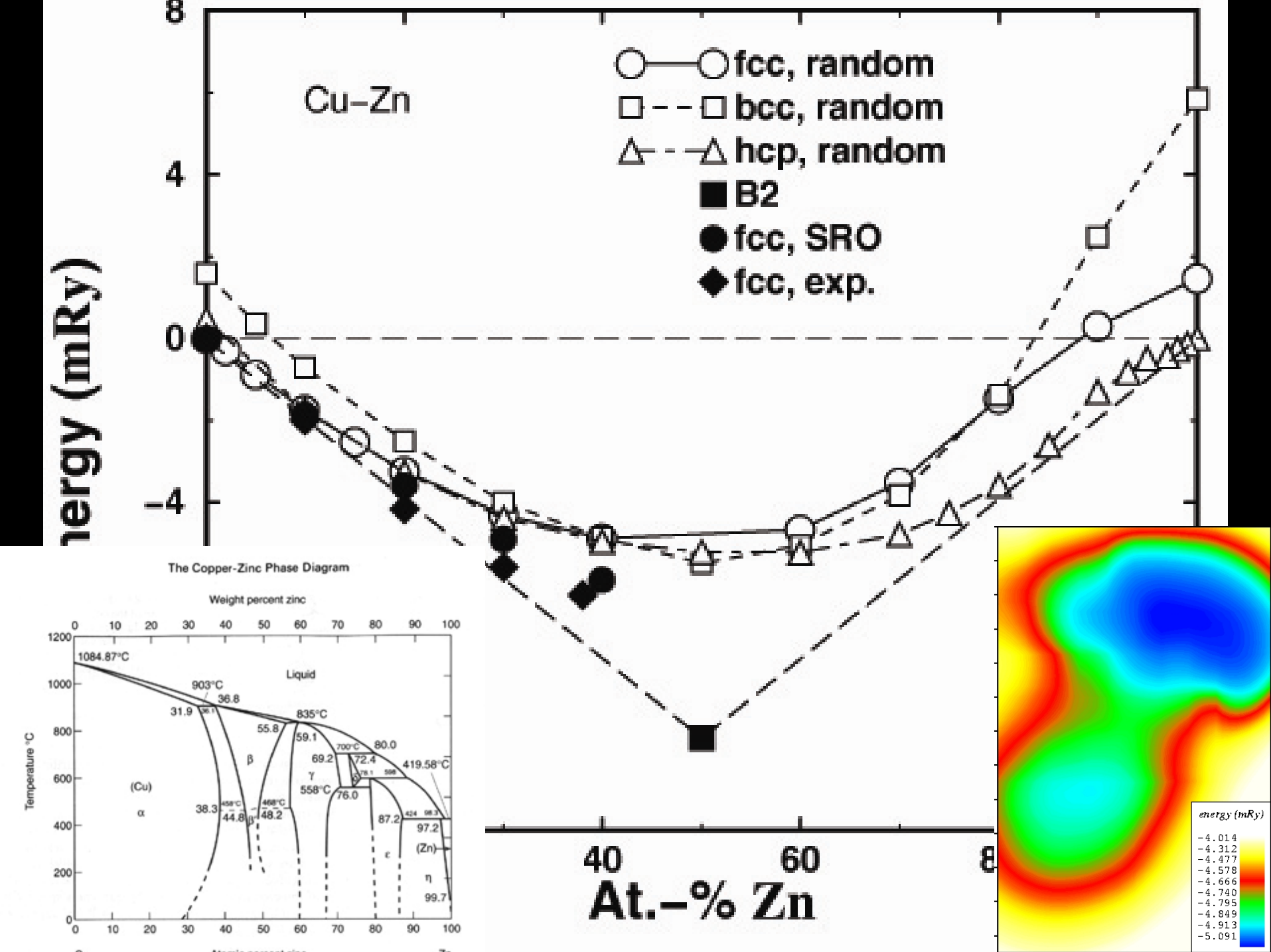
Cu–Zn
fcc, random
bcc, random
hcp, random
B2
fcc, SRO
fcc, exp.
8
4
0
−4
ergy (mRy)
40
60
At.–% Zn
The Copper-Zinc Phase Diagram
Weight percent zinc
Temperature °C
1084.87°C
Liquid
903°C
36.8
31.9
835°C
55.8
59.1
80.0
69.2
72.4
419.58°C
700°C
558°C
76.0
(Cu)
α
β
γ
38.3
44.8
48.2
87.2
97.2
(Zn)
ε
η
99.7
energy (mRy)
-4.014
-4.312
-4.477
-4.578
-4.666
-4.740
-4.795
-4.849
-4.913
-5.091

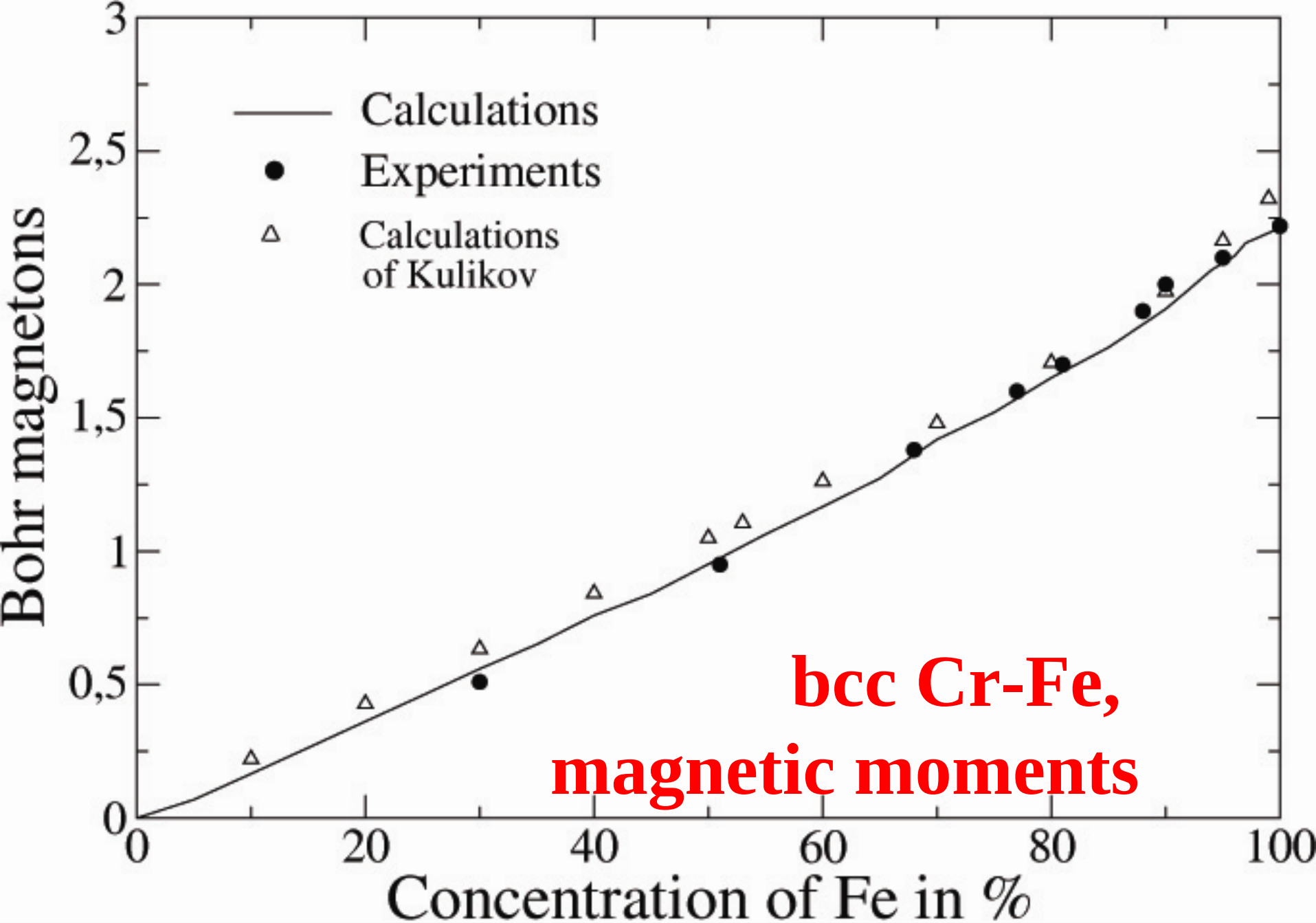
Calculations
Experiments
Calculations
of Kulikov
Bohr magnetons
Concentration of Fe in %
0
0,5
1
1,5
2
2,5
3
0
20
40
60
80
100
bcc Cr-Fe,
magnetic moments

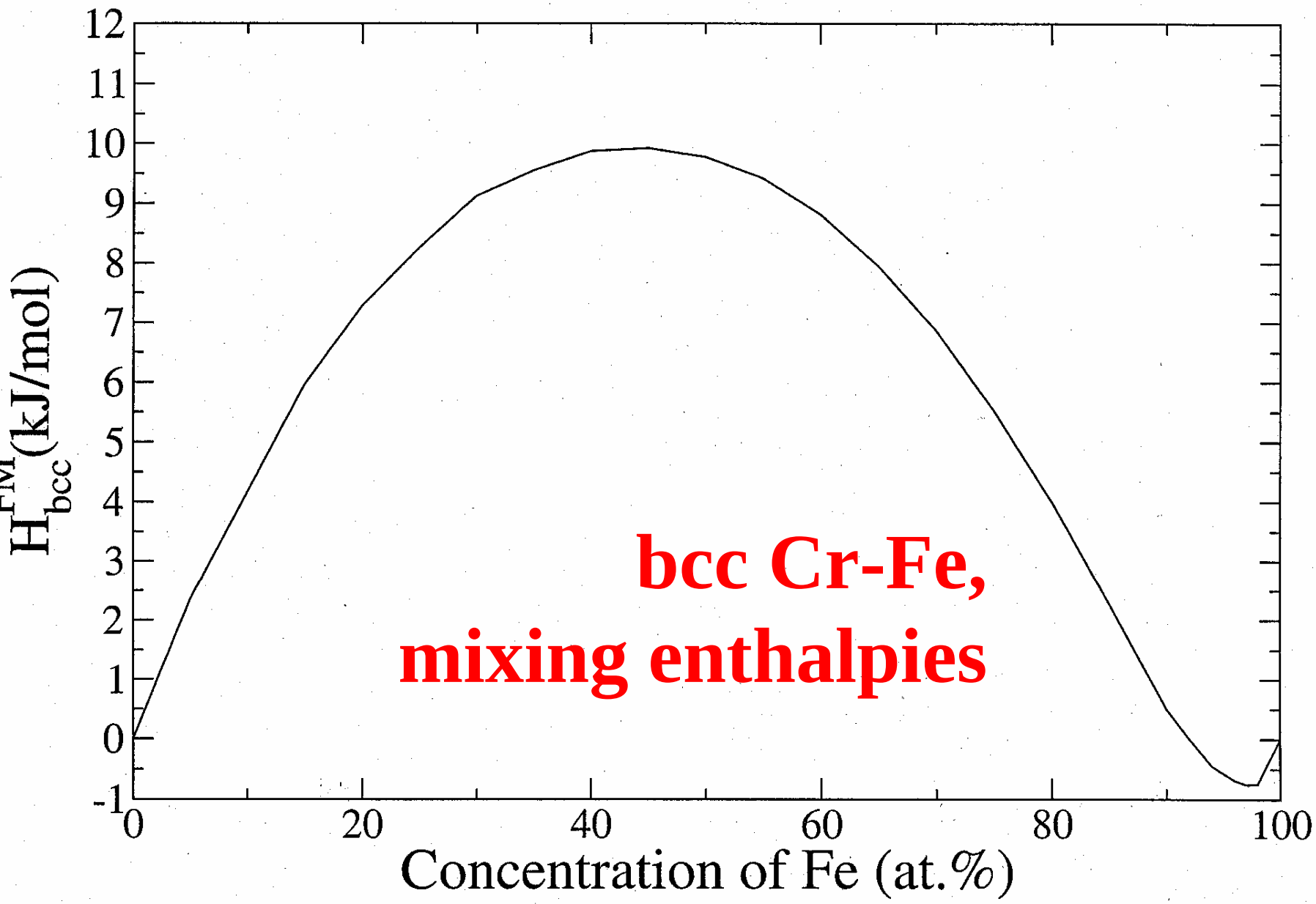

P. Olsson, I. A. Abrikosov, L. Vitos, and J. Wallenius, J. Nucl. Mater. 321, 84 (2003)

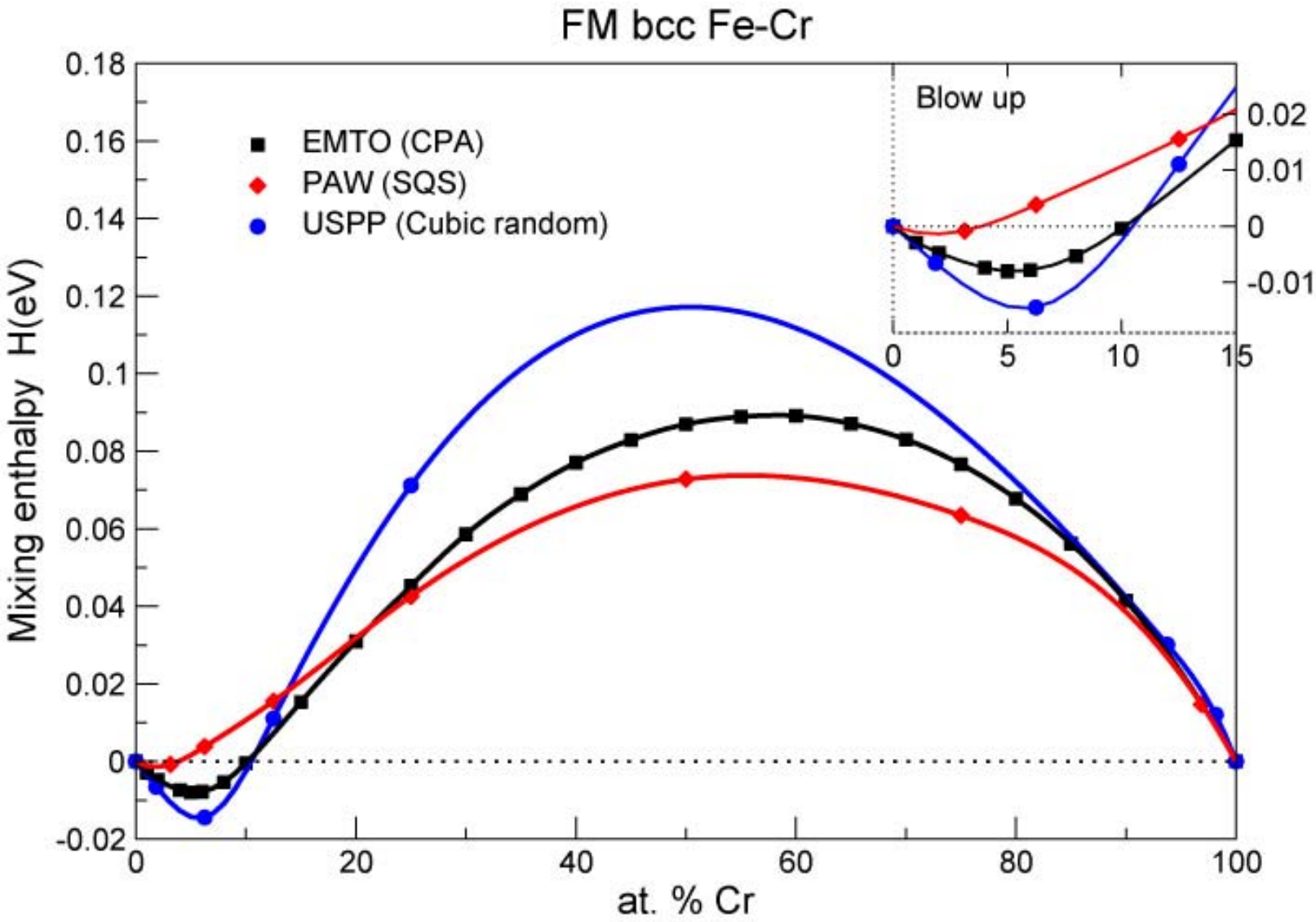

P. Olsson, I. A. Abrikosov, and J. Wallenius, Phys. Rev. B 73, 104416 (2006)

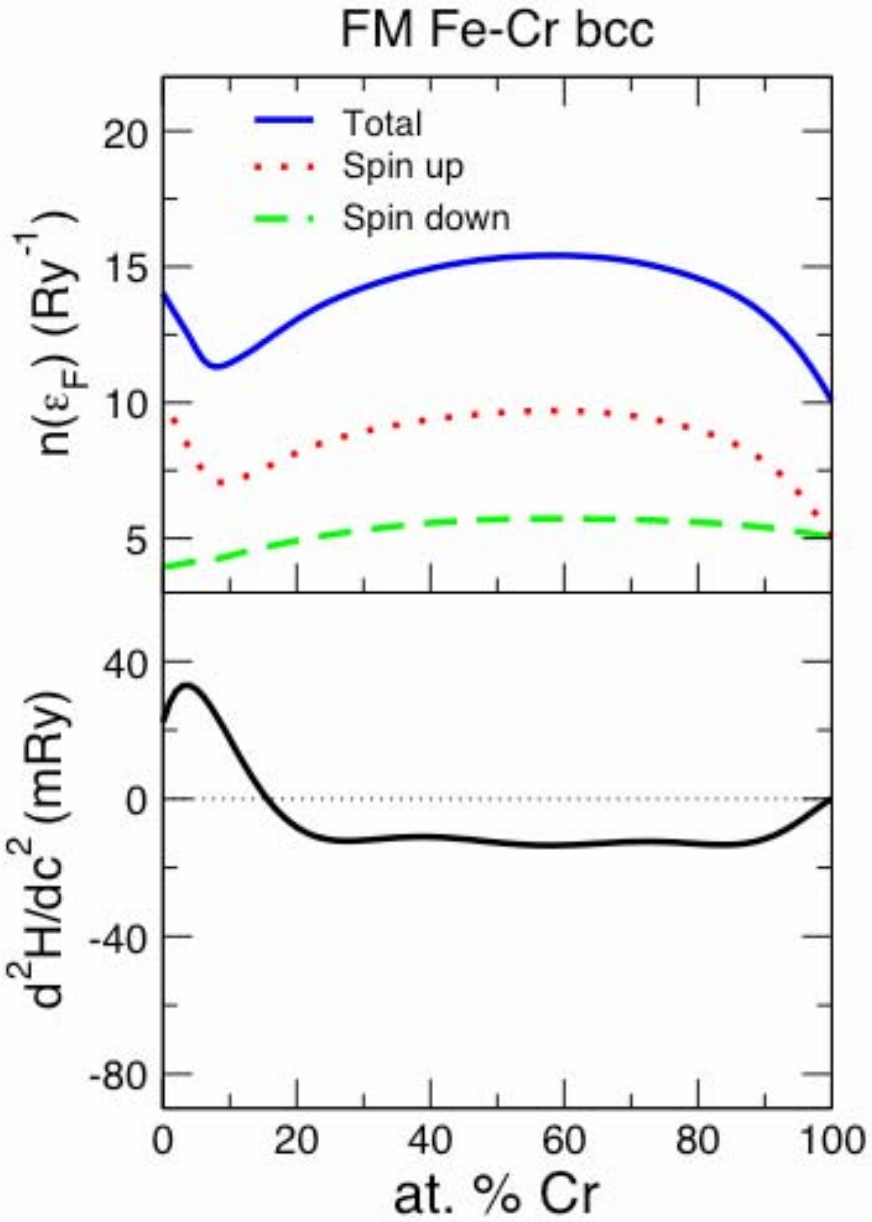

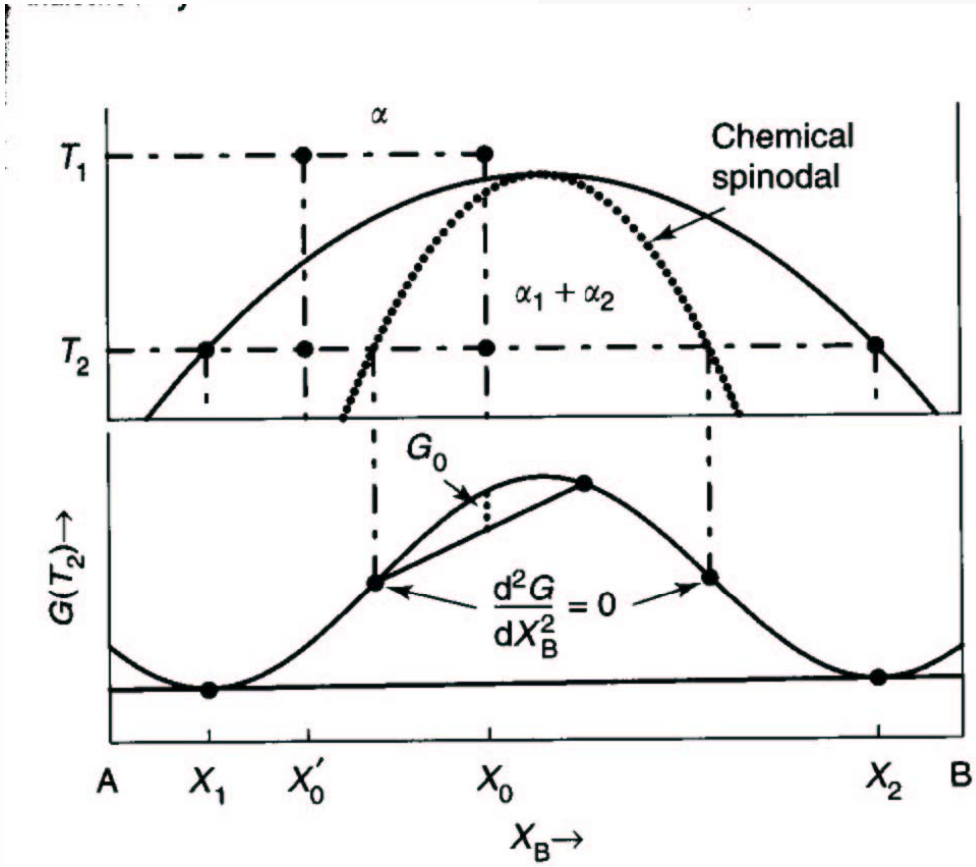

Figure 9 (a) Schematic phase diagram and (b) free energy vs composition diagram for alloys between the spinodal points which are unstable and can decompose into two coherent phases α_1 and α_2 without overcoming an activation energy barrier. Alloys between the miscibility gap and the spinodal are metastable and can decompose only after nucleation of the other phase.

$$F = -k_B T \ln Z \qquad Z = \sum_s \exp\left(-\frac{E_s}{kT}\right)$$

$$\vec{\sigma}_s = \{\sigma_i\} \qquad \sigma_i = \begin{cases} 1 & \text{if site } i \text{ is occupied by atom } A \\ -1 & \text{otherwise} \end{cases}$$

$$\langle \sigma_i \sigma_j \rangle^s, \quad \langle \sigma_i \sigma_j \sigma_k \rangle^s, \ldots$$

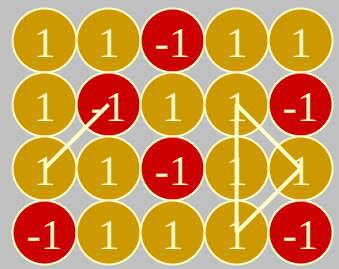

$$E_{tot} = V^{(0)} + V^{(1)} \langle \sigma \rangle +$$

$$\sum_s V^{(2,s)} \langle \sigma_i \sigma_j \rangle + \sum_s V^{(3,s)} \langle \sigma_i \sigma_j \sigma_k \rangle + \ldots$$

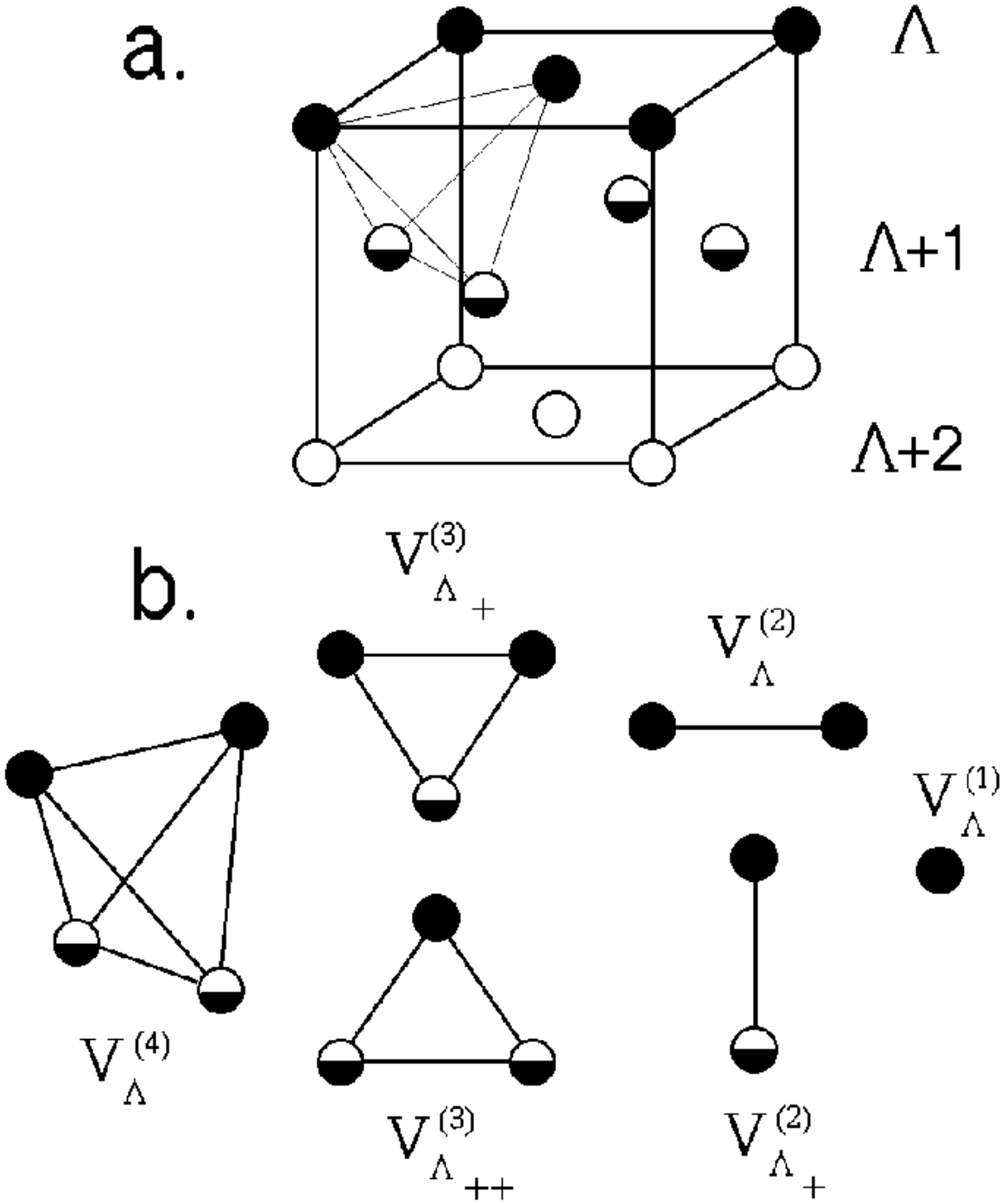
a.
Λ
Λ+1
Λ+2
b.
$V^{(3)}_{\Lambda+}$
$V^{(2)}_{\Lambda}$
$V^{(1)}_{\Lambda}$
$V^{(4)}_{\Lambda}$
$V^{(3)}_{\Lambda++}$
$V^{(2)}_{\Lambda+}$

Calculations of effective interatomic potentials

The generalized perturbation method

1. Calculate electronic structure of a random alloy (for example, use the CPA): $\tilde{g}\,,\ t^{A(B)}$

2. $$E_{one} = E_{one}(c) + \frac{1}{2}\sum_{RR'} V_{RR'} \left\langle \sigma_i \sigma_j \right\rangle^{(RR')} \ldots$$

-determine a perturbation of the band energy due to small varioations of the correlation functions

where the effective interatomic interactions are given by an analytical formula:

$$V_{RR'} = -\frac{1}{\pi}\int dE \left\{ t^A_R \gamma_{RR'} t^B_{R'} \gamma_{R'R} t^A_R \right\}$$

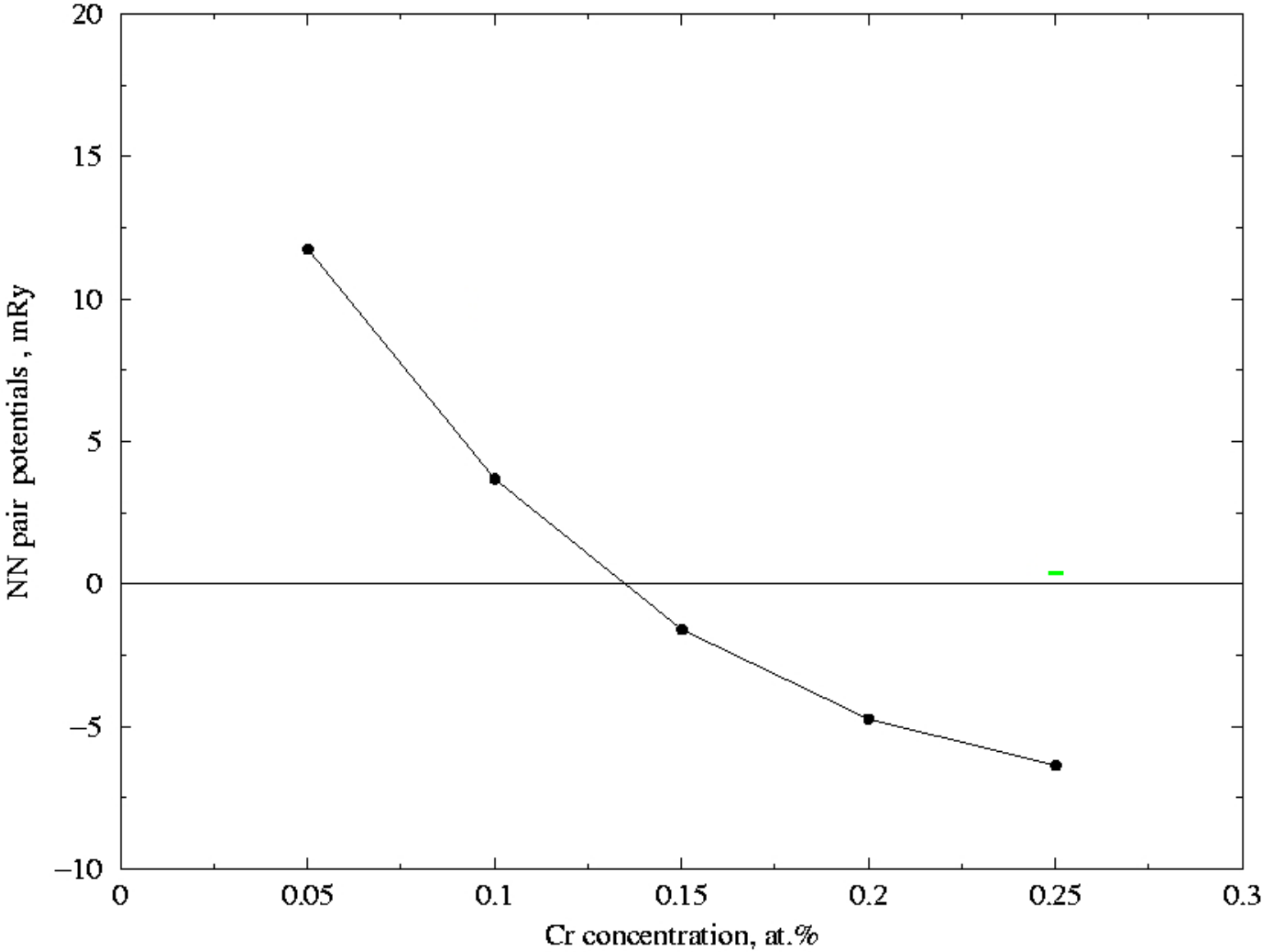
20
15
10
5
0
−5
−10
0
0.05
0.1
0.15
0.2
0.25
0.3
NN pair potentials , mRy
Cr concentration, at.%

Calculations of effective interatomic potentials

The Connolly-Williams method

1. Choose structures fcc $L1_2$ $L1_0$ DO22

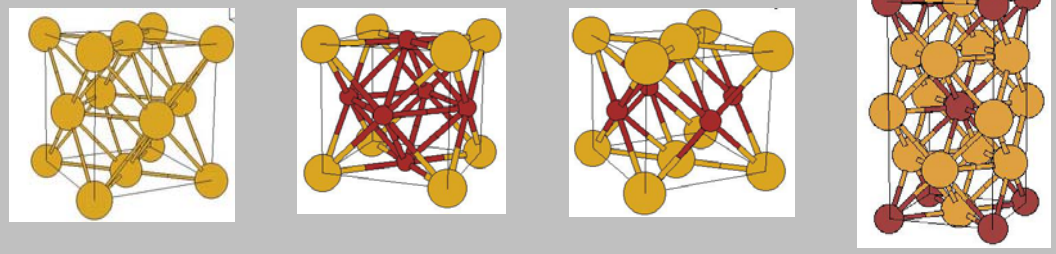

with predefined correlation functions

$$\left[\left\langle\sigma_i\sigma_j\right\rangle^{(2,1)}, \left\langle\sigma_i\sigma_j\right\rangle^{(2,2)}, \left\langle\sigma_i\sigma_j\sigma_k\right\rangle^{(3,1)}, \ldots\right]$$

2. Calculate E_{tot}: E(fcc) E($L1_2$) E($L1_0$) E(DO22)

$$E_{tot} = V^{(0)} + V^{(1)}\left\langle\sigma\right\rangle + \sum_s V^{(2,s)}\left\langle\sigma_i\sigma_j\right\rangle \ldots$$

If $N_{pot} \le N_{str}$ then $\{V\}$ are found by L.S.M: $\sum_m \left[E_m - \sum_f \left\langle\ldots\right\rangle^f V_f\right]^2 = \min$

The Monte Carlo method

Calculations of averages at temperature *T*:

$$\langle A \rangle = \frac{\sum_s A_s \exp\left(-\frac{E_s}{k_B T}\right)}{Z}$$

Create the Marcov chain of configurations:

$$P_s = \frac{1}{Z}\exp\left(-\frac{E_s}{k_B T}\right)$$

Balance at the equilibrium state:

$$W(s \to s')\exp\left(-\frac{E_s}{k_B T}\right) = W(s' \to s)\exp\left(-\frac{E_{s'}}{k_B T}\right)$$

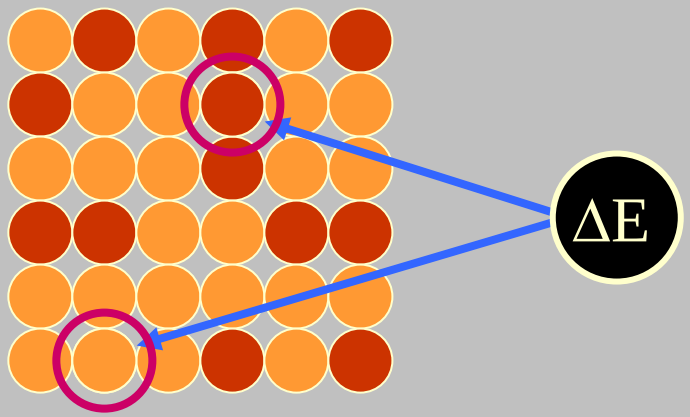

$$\begin{cases} \Delta E \le 0 \\ \Delta E > 0 \quad \exp\left[-\frac{\Delta E}{k_B T}\right] > r \quad (0 \le r \le 1) \end{cases}$$

Atoms exchanged

Multiscale simulations of radiation damage in Fe-Cr alloys
J. Wallenius, I. A. Abrikosov, P. Olsson *et al.*,
J. Nucl. Mater. **329-333**, 1175 (2004).

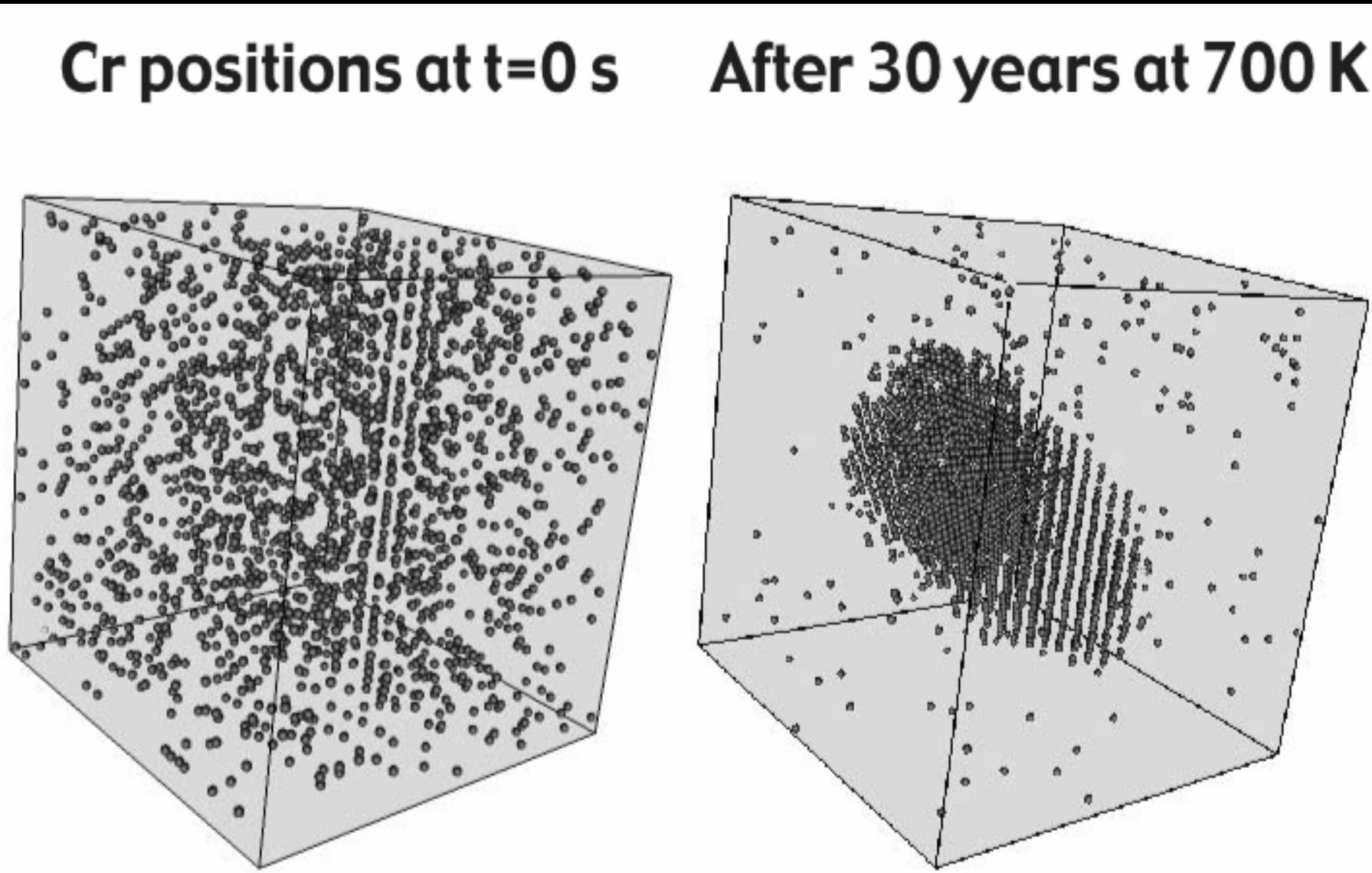

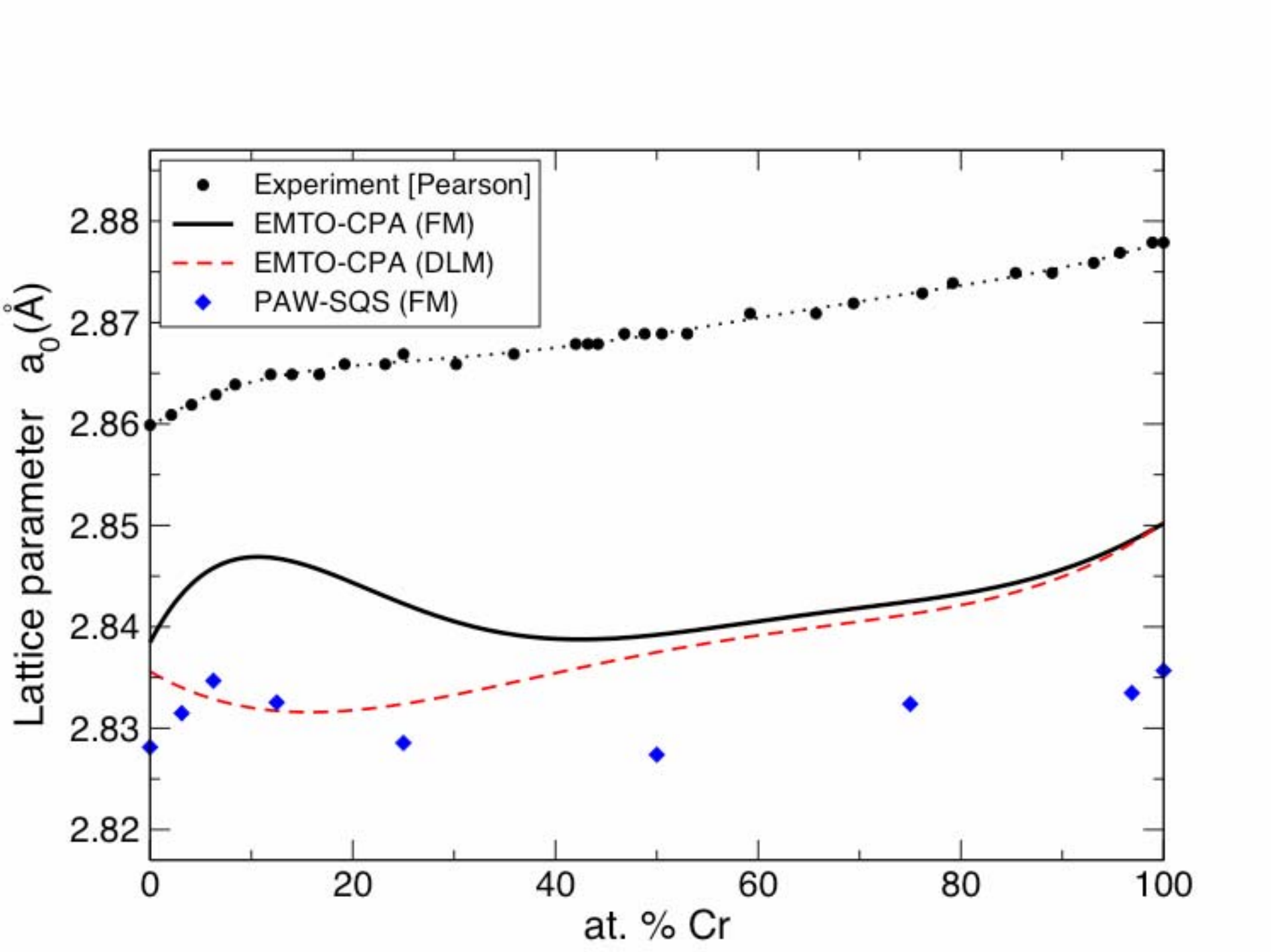
Experiment [Pearson]
EMTO-CPA (FM)
EMTO-CPA (DLM)
PAW-SQS (FM)
Lattice parameter a_0(Å)
2.88
2.87
2.86
2.85
2.84
2.83
2.82
0
20
40
60
80
100
at. % Cr

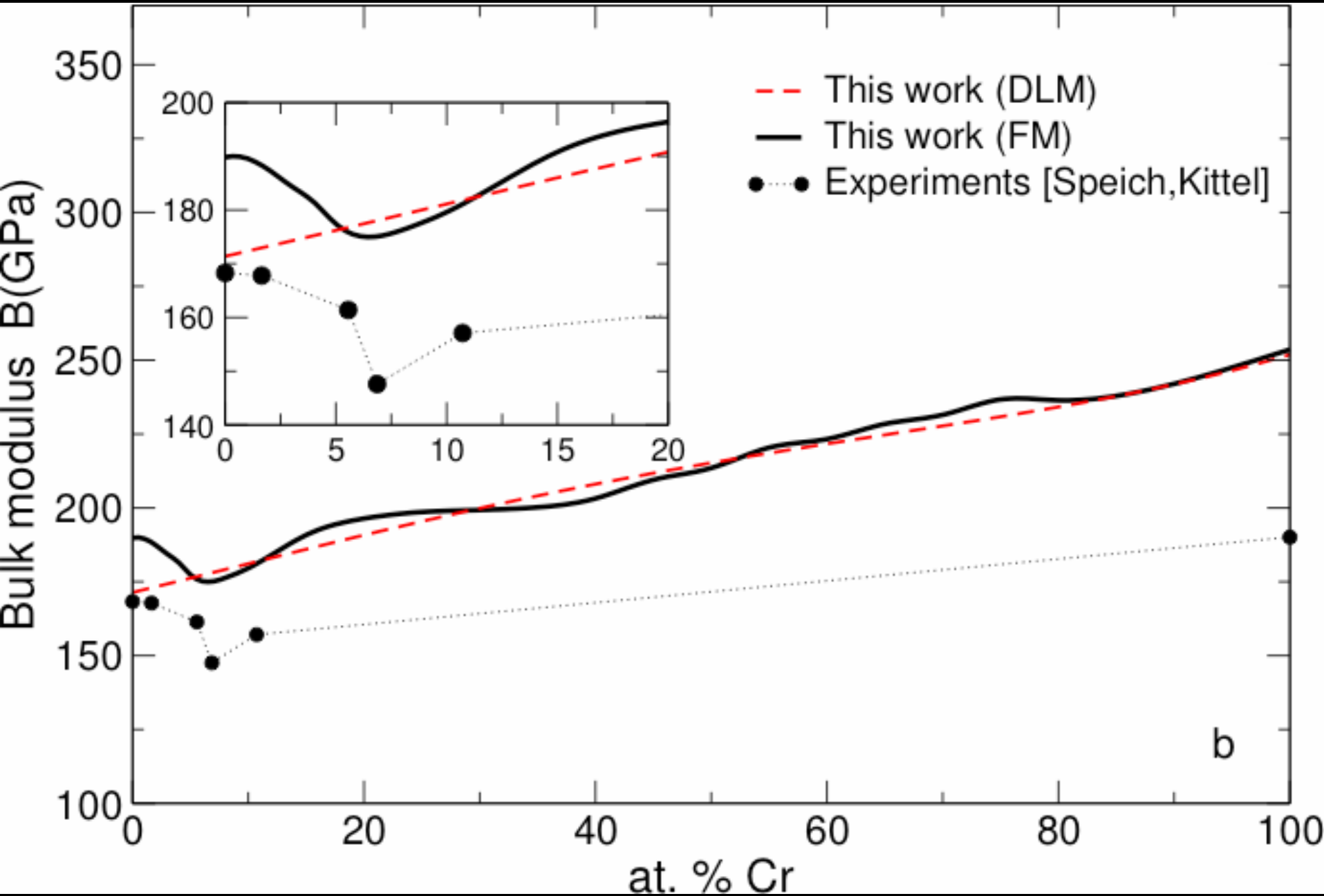
This work (DLM)
This work (FM)
Experiments [Speich,Kittel]
Bulk modulus B(GPa)
at. % Cr
b
350
300
250
200
150
100
0
20
40
60
80
100
200
180
160
140
0
5
10
15
20

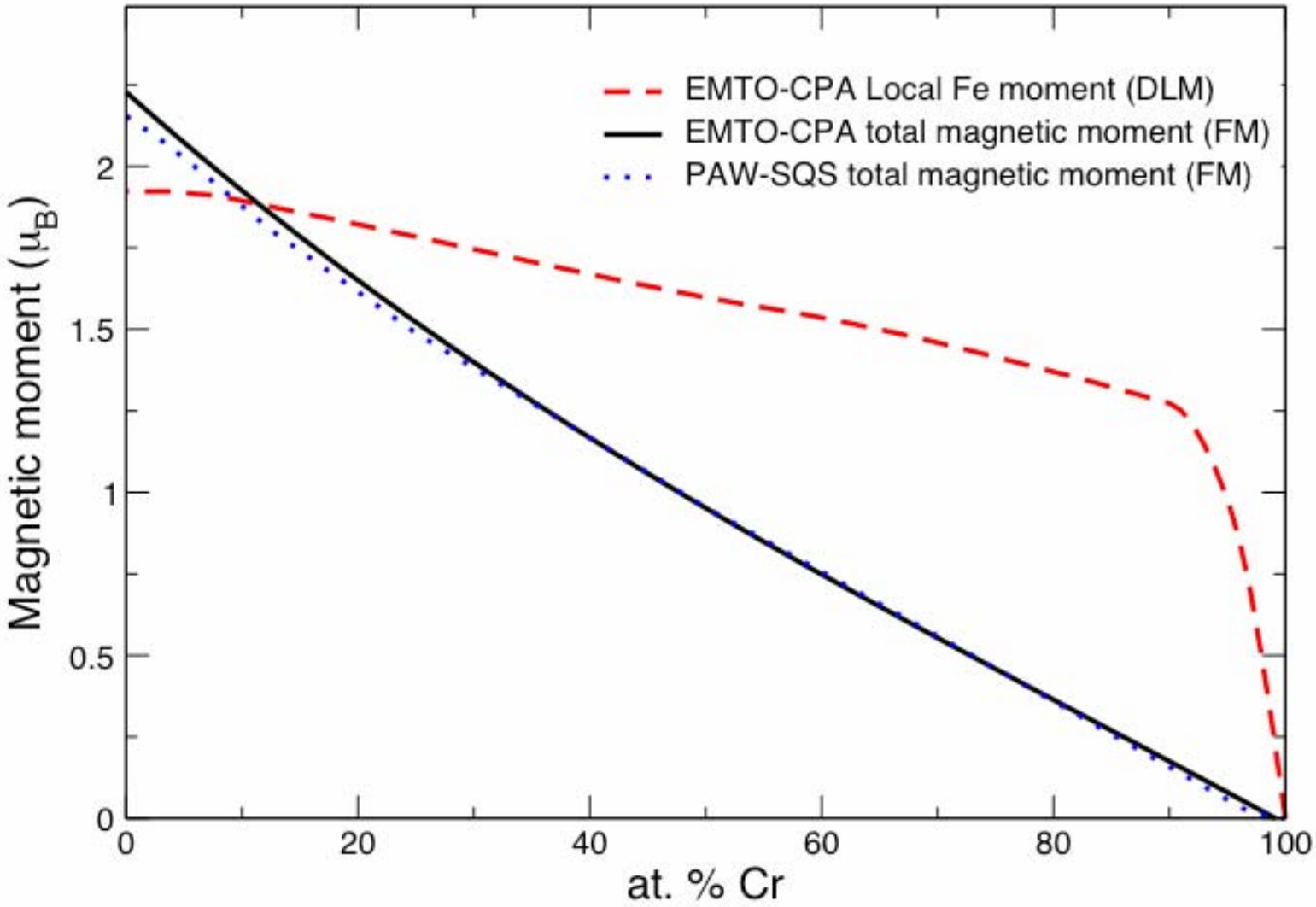
EMTO-CPA Local Fe moment (DLM)
EMTO-CPA total magnetic moment (FM)
PAW-SQS total magnetic moment (FM)
Magnetic moment (μ_B)
0
0.5
1
1.5
2
0
20
40
60
80
100
at. % Cr

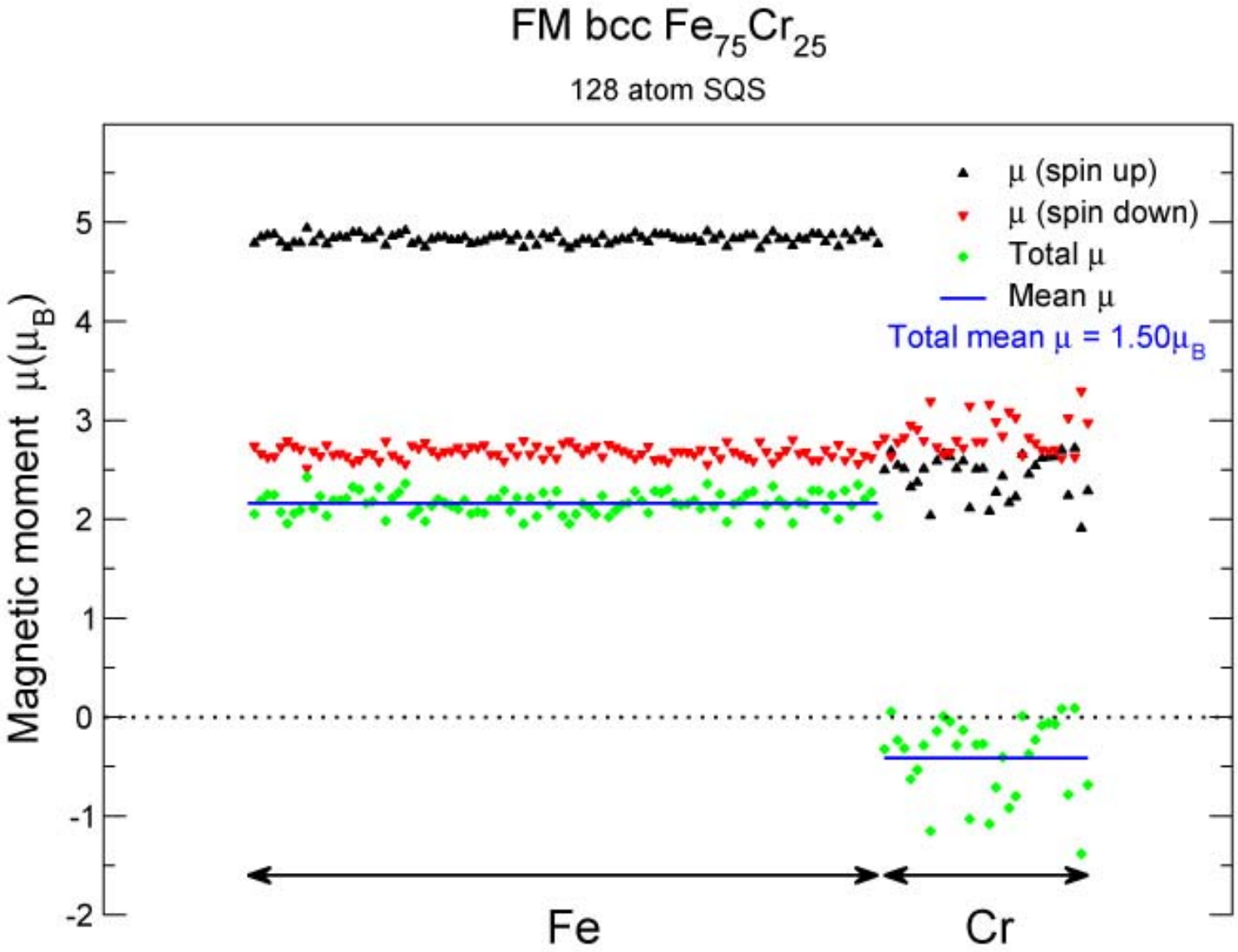
FM bcc $Fe_{75}Cr_{25}$
128 atom SQS
μ (spin up)
μ (spin down)
Total μ
Mean μ
Total mean μ = 1.50μ_B
Magnetic moment μ(μ_B)
5
4
3
2
1
0
-1
-2
Fe
Cr

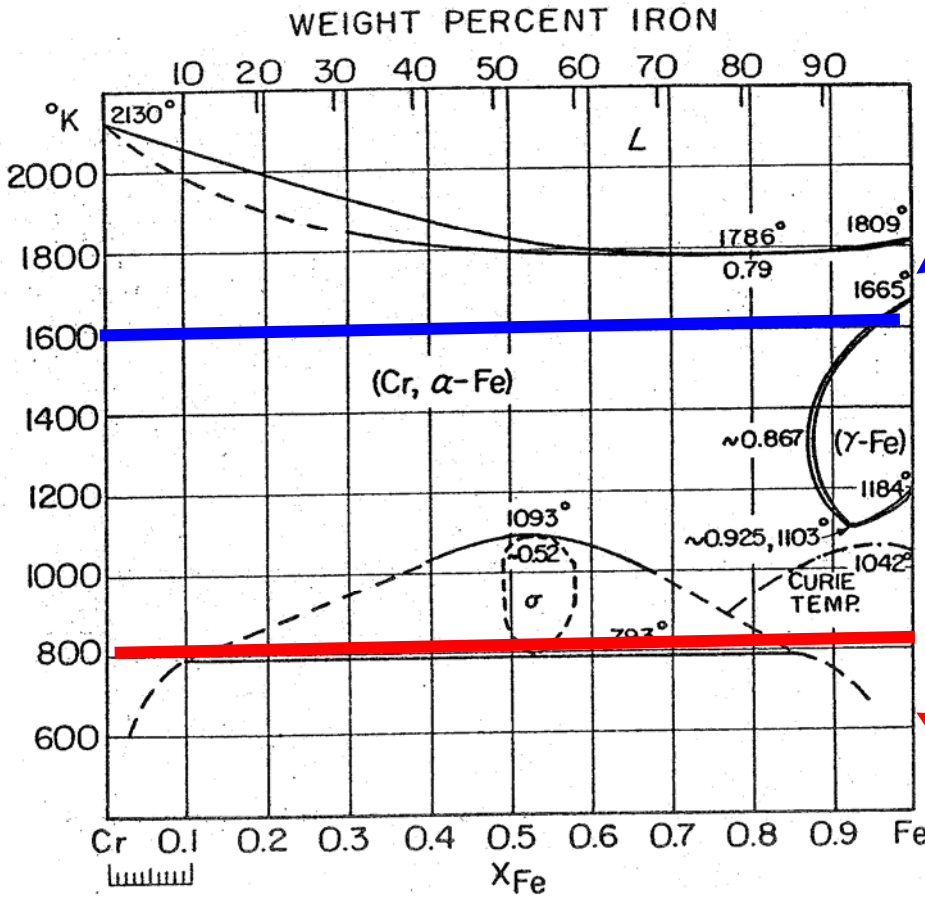

CHROMIUM - IRON SYSTEM, 1600 °K

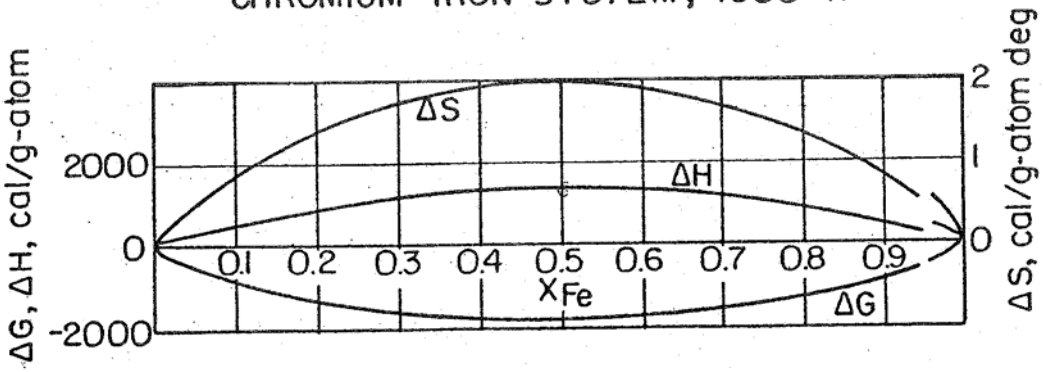

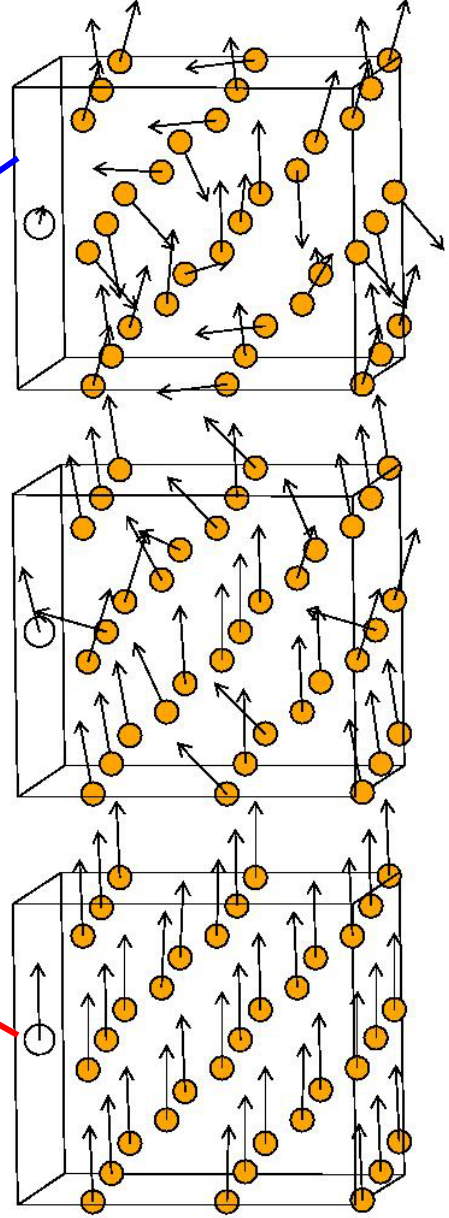

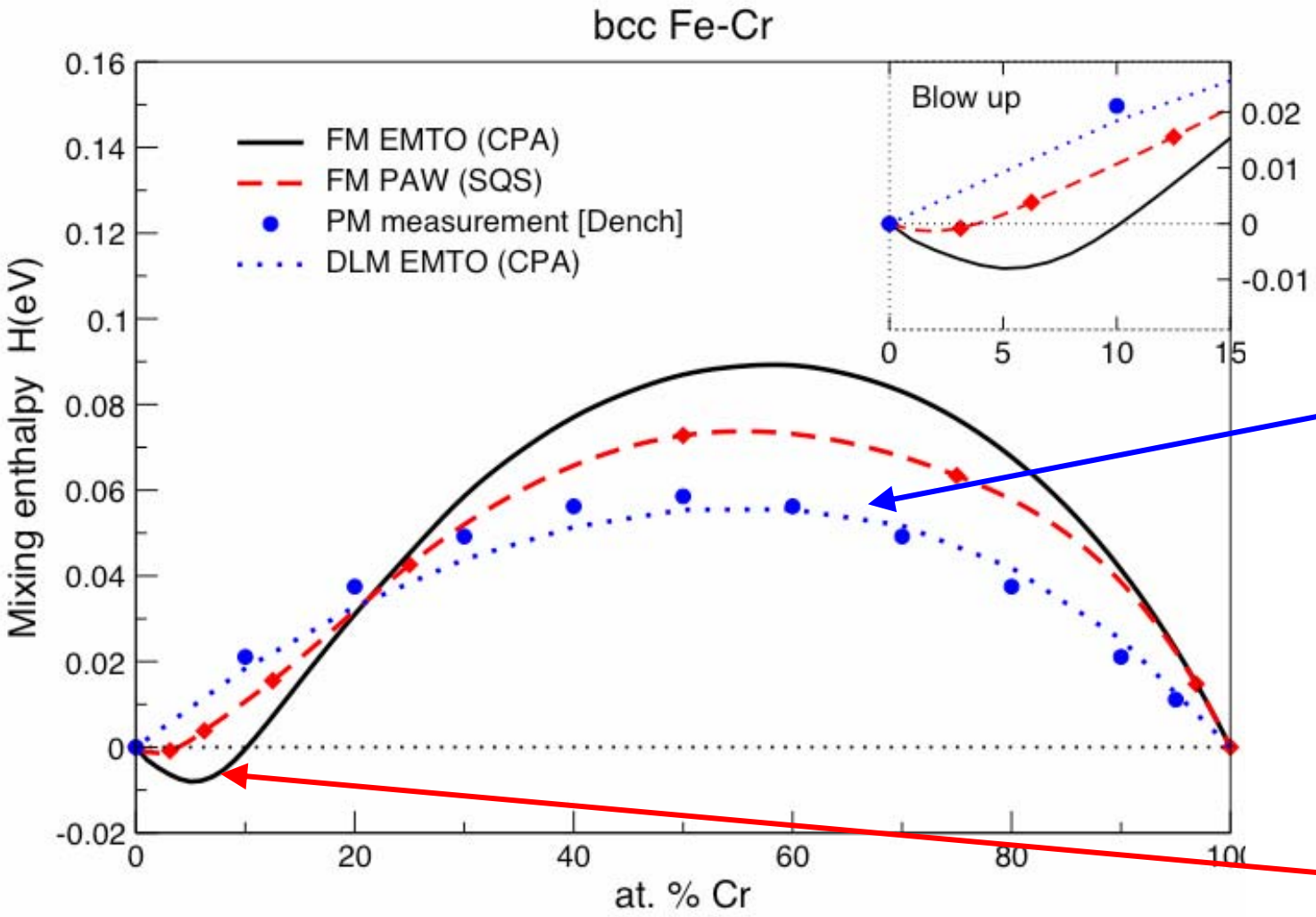
bcc Fe-Cr
Mixing enthalpy H(eV)
at. % Cr
FM EMTO (CPA)
FM PAW (SQS)
PM measurement [Dench]
DLM EMTO (CPA)
Blow up
0.16
0.14
0.12
0.1
0.08
0.06
0.04
0.02
0
-0.02
0
20
40
60
80
0.02
0.01
0
-0.01
0
5
10
15

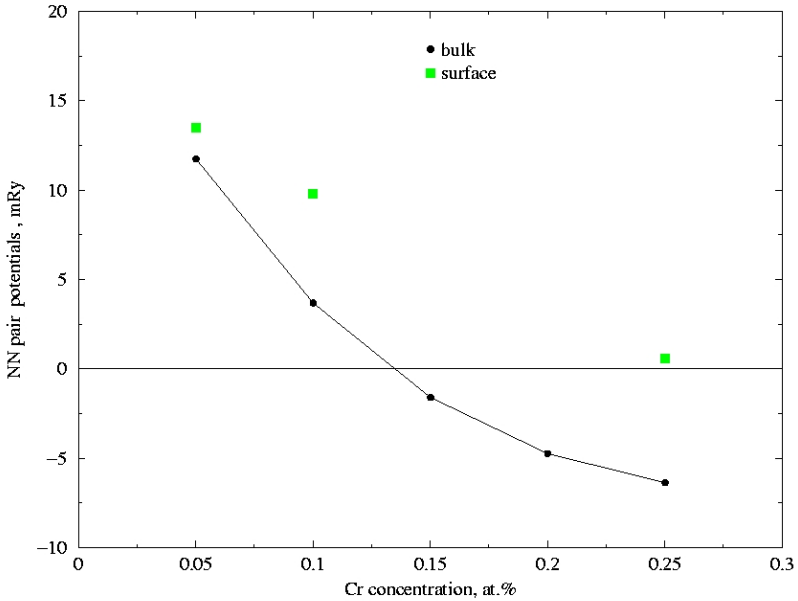
bulk
surface
NN pair potentials , mRy
Cr concentration, at.%

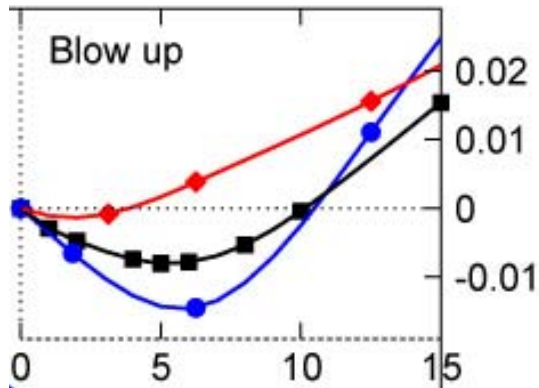
Blow up

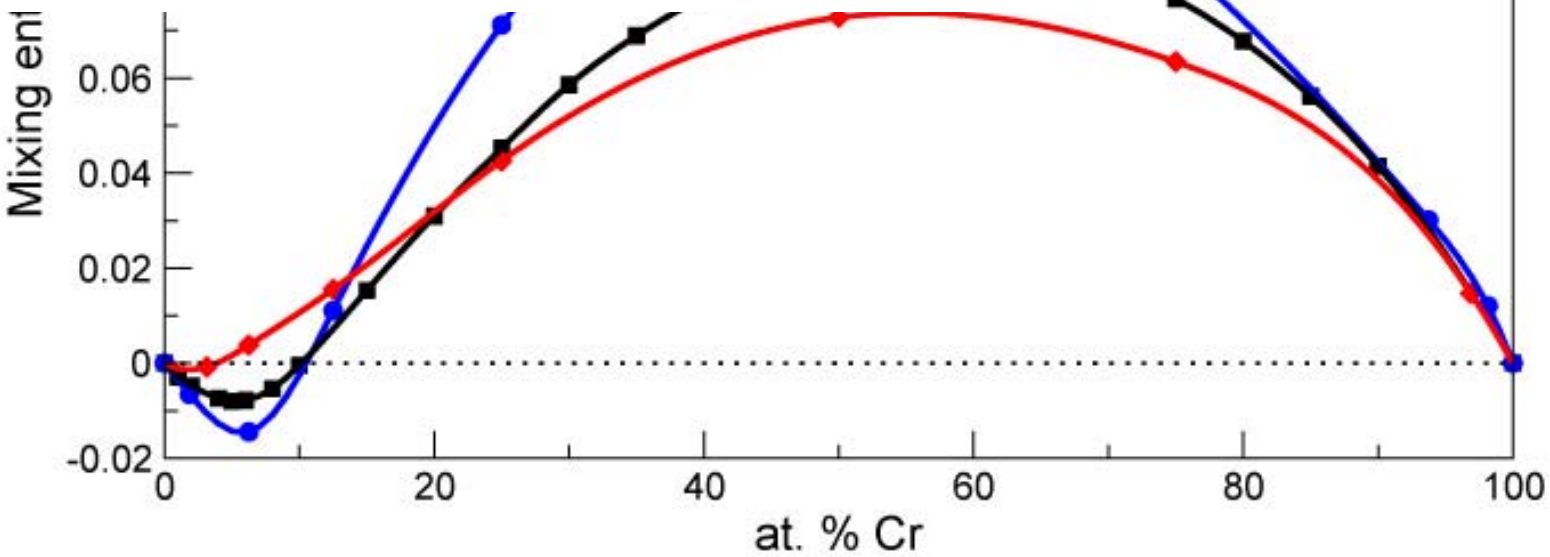
Mixing en
at. % Cr

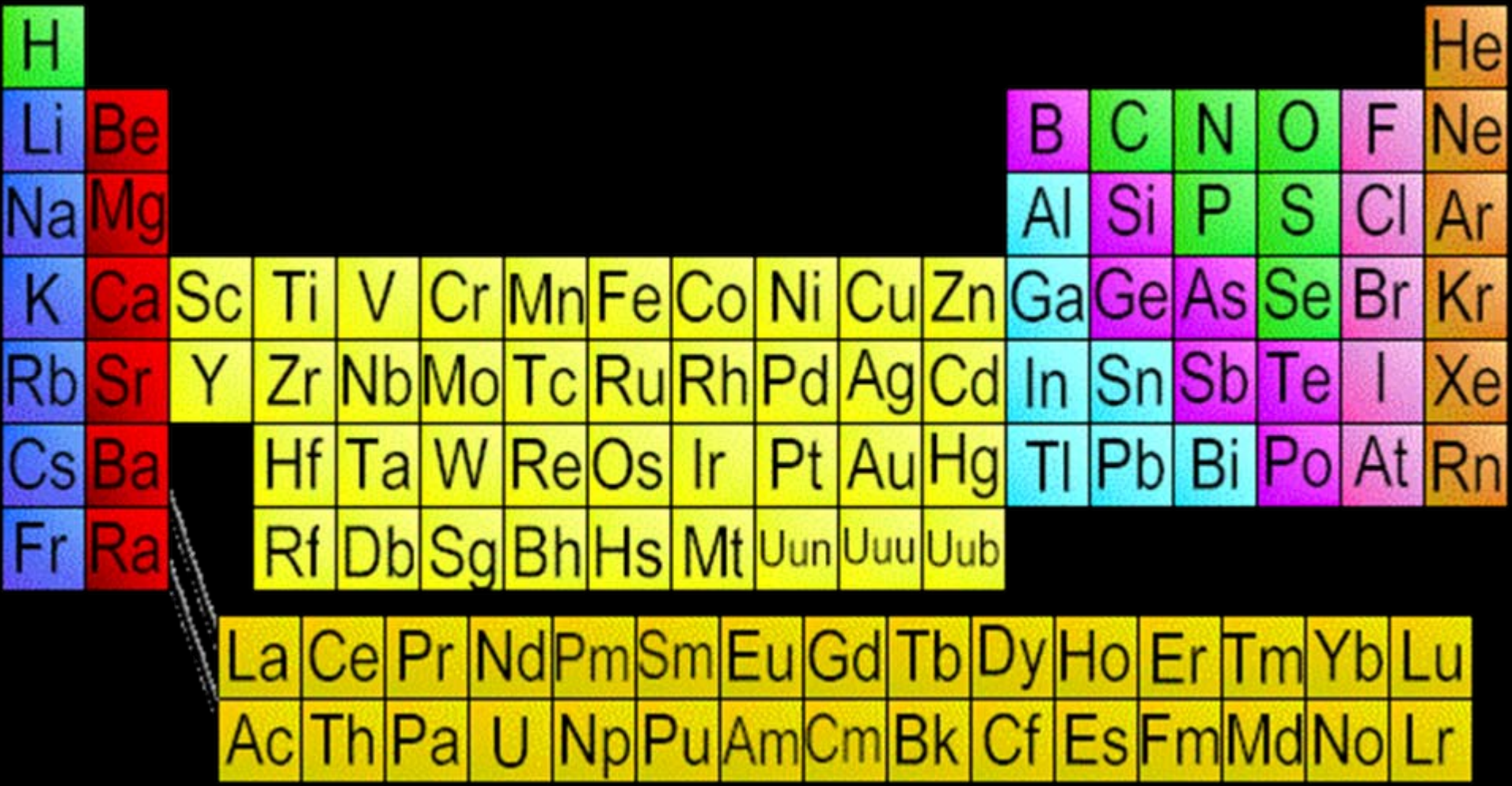
H
He
Li
Be
B
C
N
O
F
Ne
Na
Mg
Al
Si
P
S
Cl
Ar
K
Ca
Sc
Ti
V
Cr
Mn
Fe
Co
Ni
Cu
Zn
Ga
Ge
As
Se
Br
Kr
Rb
Sr
Y
Zr
Nb
Mo
Tc
Ru
Rh
Pd
Ag
Cd
In
Sn
Sb
Te
I
Xe
Cs
Ba
Hf
Ta
W
Re
Os
Ir
Pt
Au
Hg
Tl
Pb
Bi
Po
At
Rn
Fr
Ra
Rf
Db
Sg
Bh
Hs
Mt
Uun
Uuu
Uub
La
Ce
Pr
Nd
Pm
Sm
Eu
Gd
Tb
Dy
Ho
Er
Tm
Yb
Lu
Ac
Th
Pa
U
Np
Pu
Am
Cm
Bk
Cf
Es
Fm
Md
No
Lr

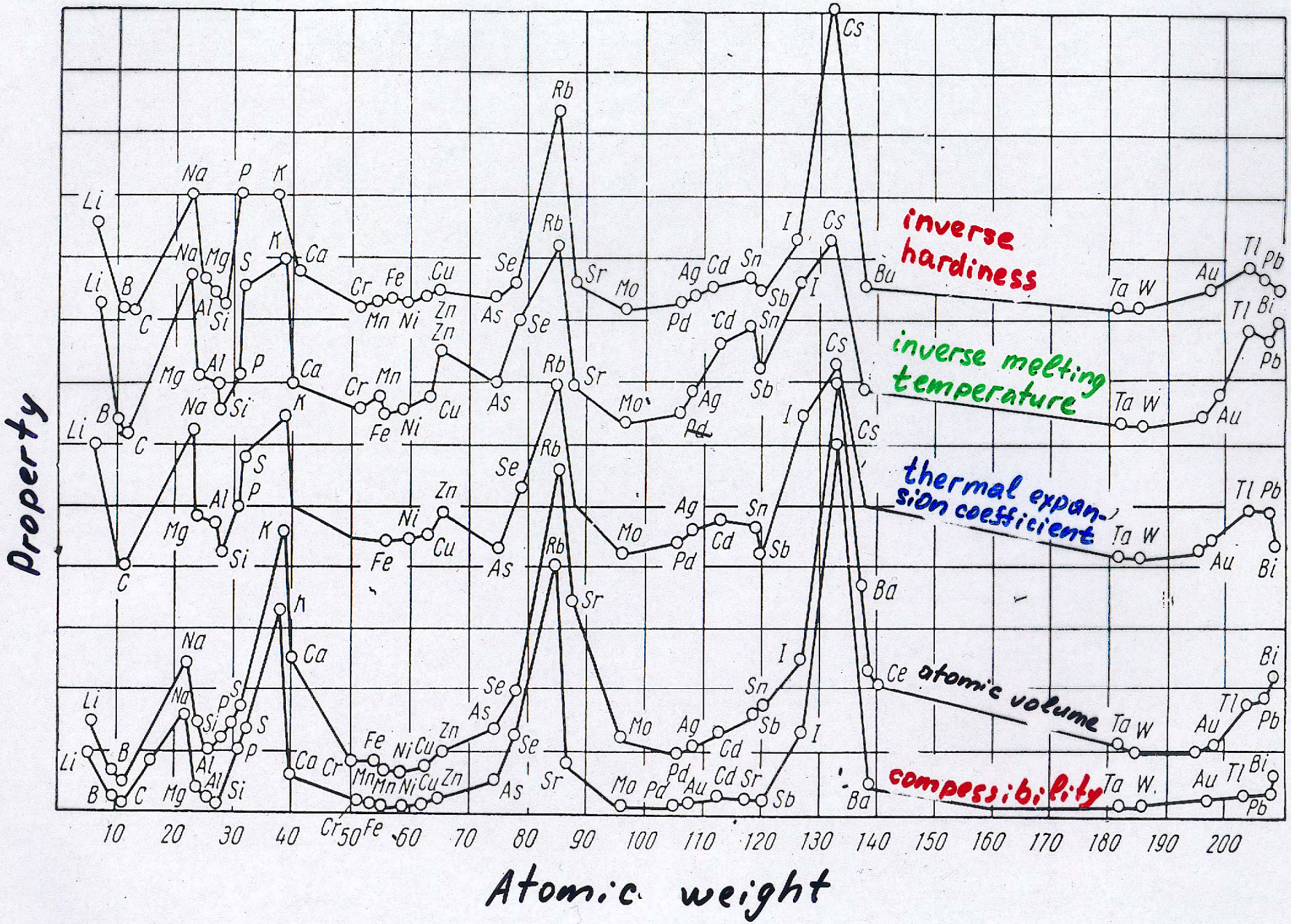
Property
inverse hardiness
inverse melting temperature
thermal expansion coefficient
atomic volume
compressibility
10 20 30 40 50 60 70 80 90 100 110 120 130 140 150 160 170 180 190 200
Atomic weight

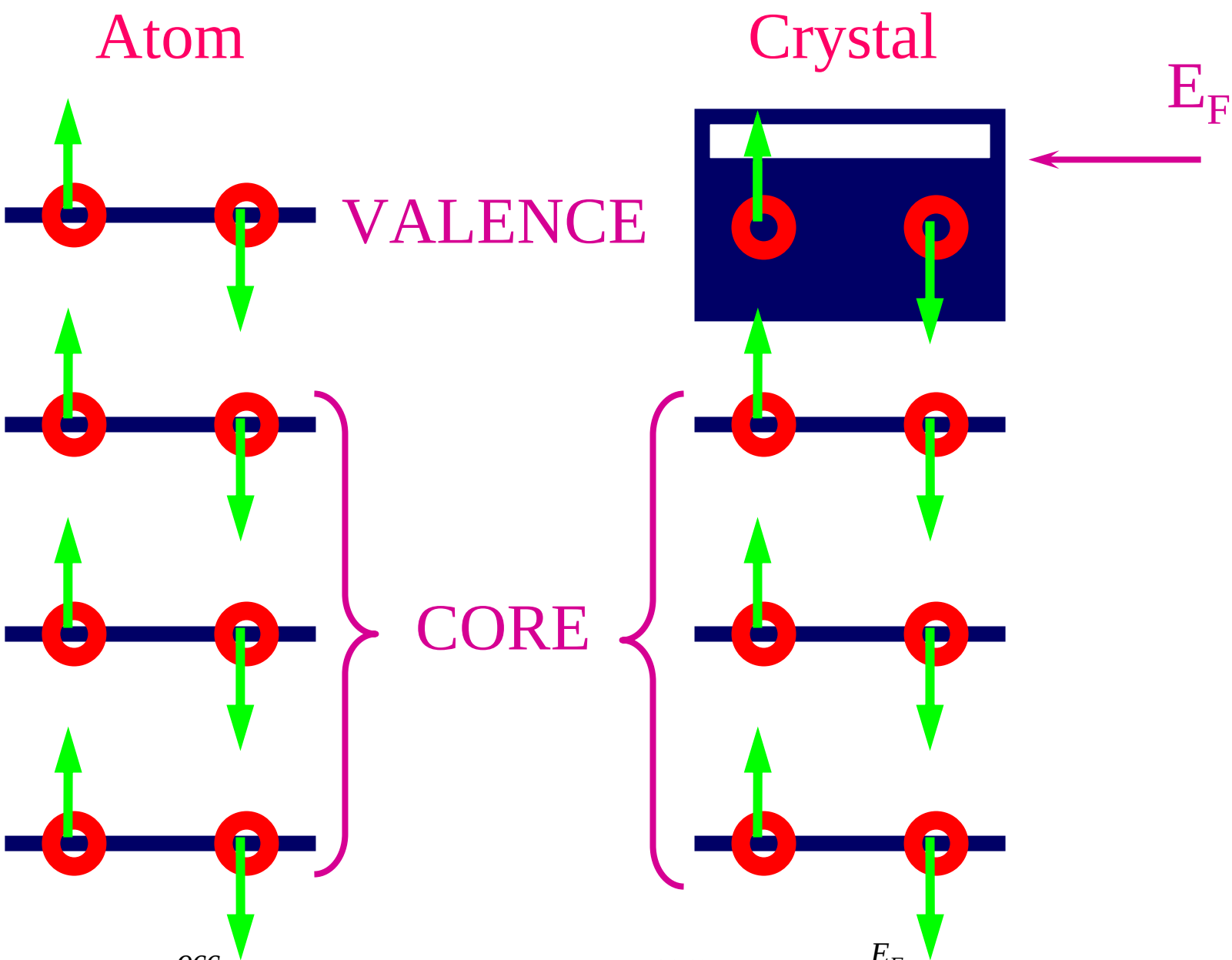
Atom
Crystal
E_F
VALENCE
CORE
$E_{tot} = \sum^{occ} E_i^{atom} n_i$
$E_{tot} = \sum^{core} E_i \, n_i + \int_{valence}^{E_F} E n(E) dE$

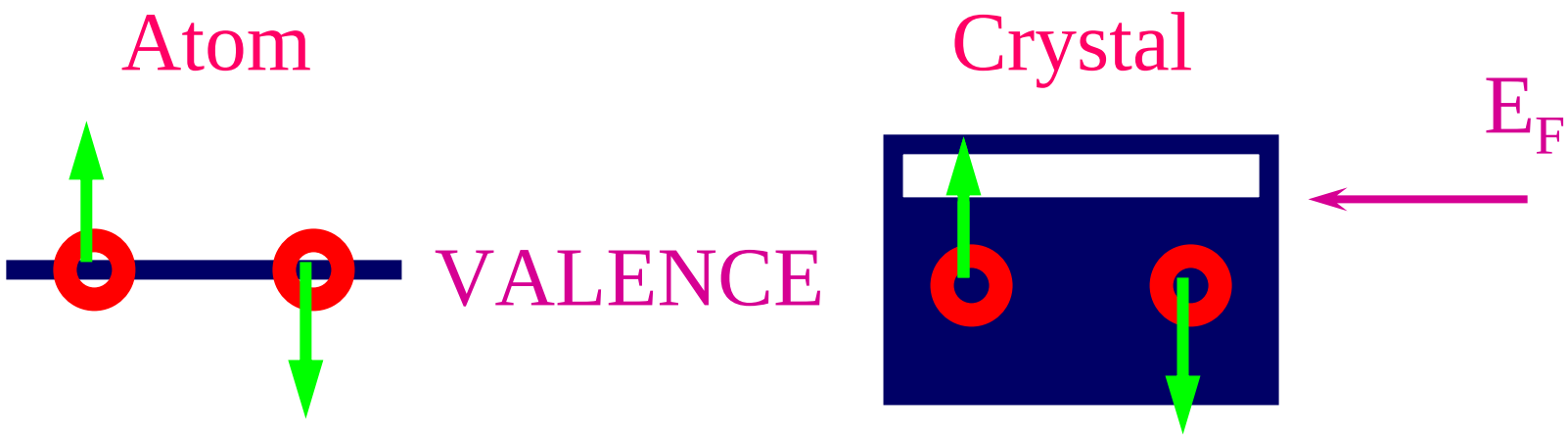

$$E_{BOND} = E_{tot}^{crystal} - E_{tot}^{atom} = \int_{valence}^{E_F} (E - E_{valence}^{atom}) n(E) dE$$

Transition metal

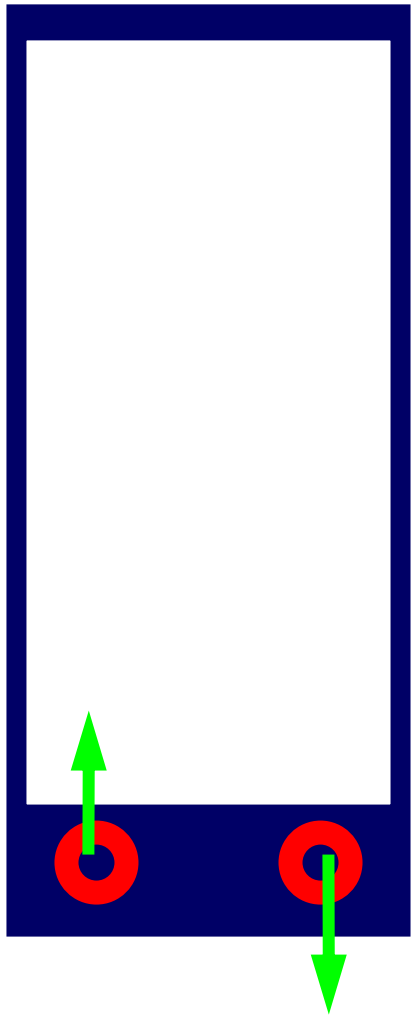

Zr

E_F

$$E_{BOND} = E_{tot}^{crystal} - E_{tot}^{atom} = \int_{valence}^{E_F} (E - E_{valence}^{atom}) n(E) dE$$

Transition metal

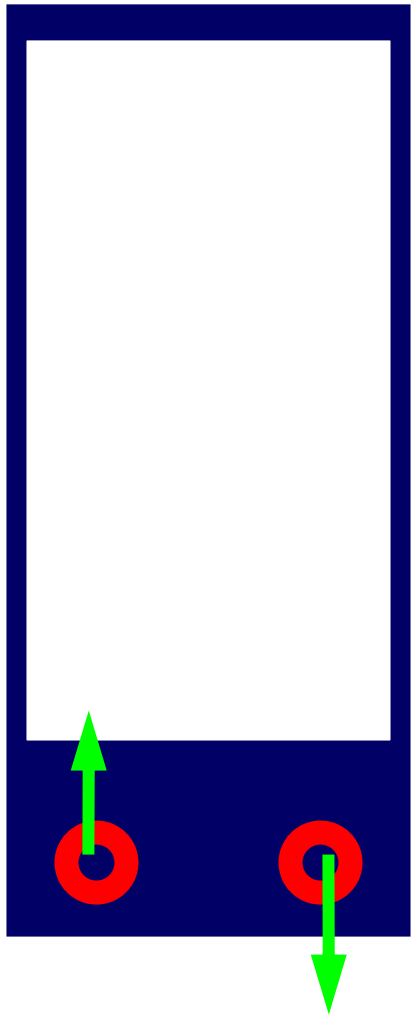

Nb

E_F

$$E_{BOND} = E_{tot}^{crystal} - E_{tot}^{atom} = \int_{valence}^{E_F} (E - E_{valence}^{atom}) n(E) dE$$

Transition metal

Mo

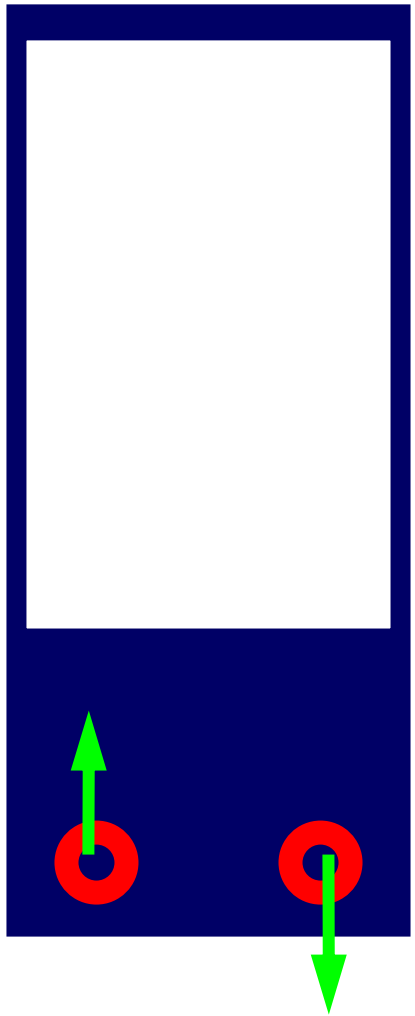

E_F

$$E_{BOND} = E_{tot}^{crystal} - E_{tot}^{atom} = \int_{valence}^{E_F} (E - E_{valence}^{atom}) n(E) dE$$

Transition metal

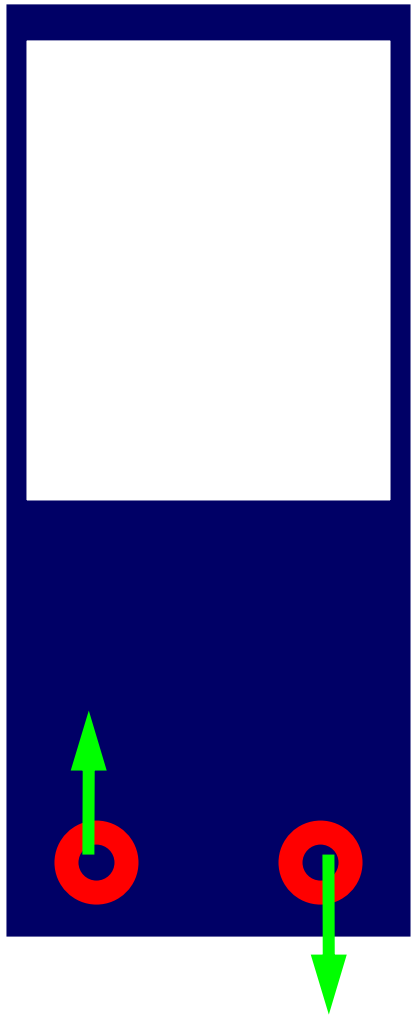

Tc

E_F

$$E_{BOND} = E_{tot}^{crystal} - E_{tot}^{atom} = \int_{valence}^{E_F} (E - E_{valence}^{atom}) n(E) dE$$

Transition metal

Ru

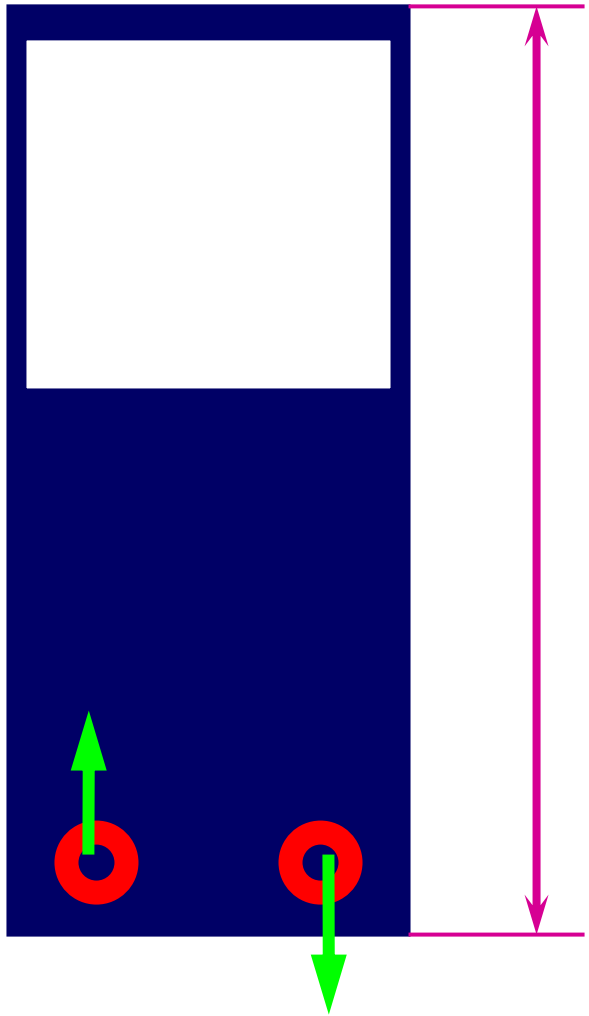

$$E_{BOND} = E_{tot}^{crystal} - E_{tot}^{atom} = \int_{valence}^{E_F} (E - E_{valence}^{atom}) n(E) dE$$

Transition metal

Ru

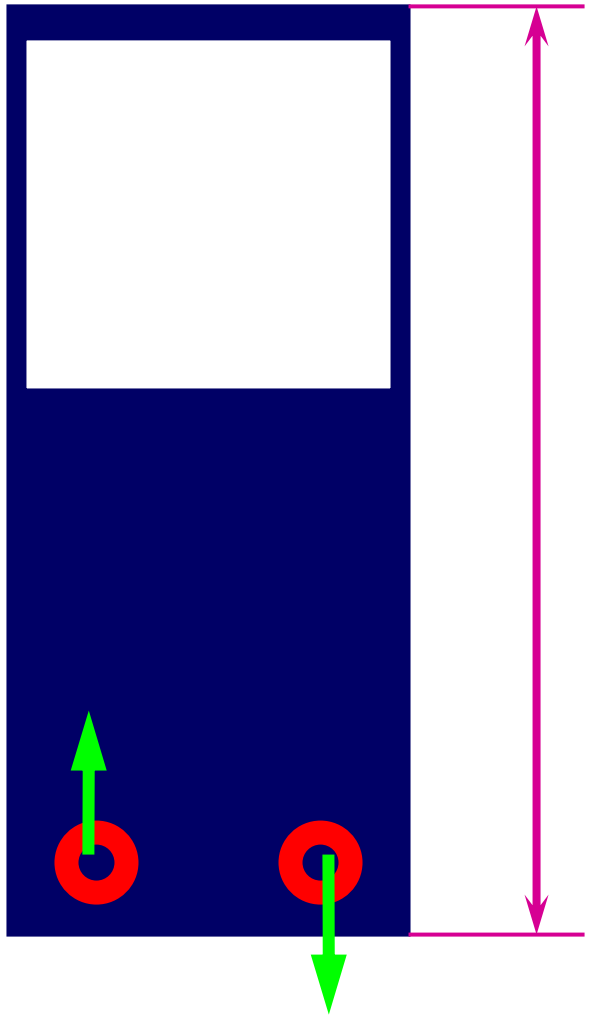

$$E_{BOND} = -\frac{1}{20} W N_d (10 - N_d)$$

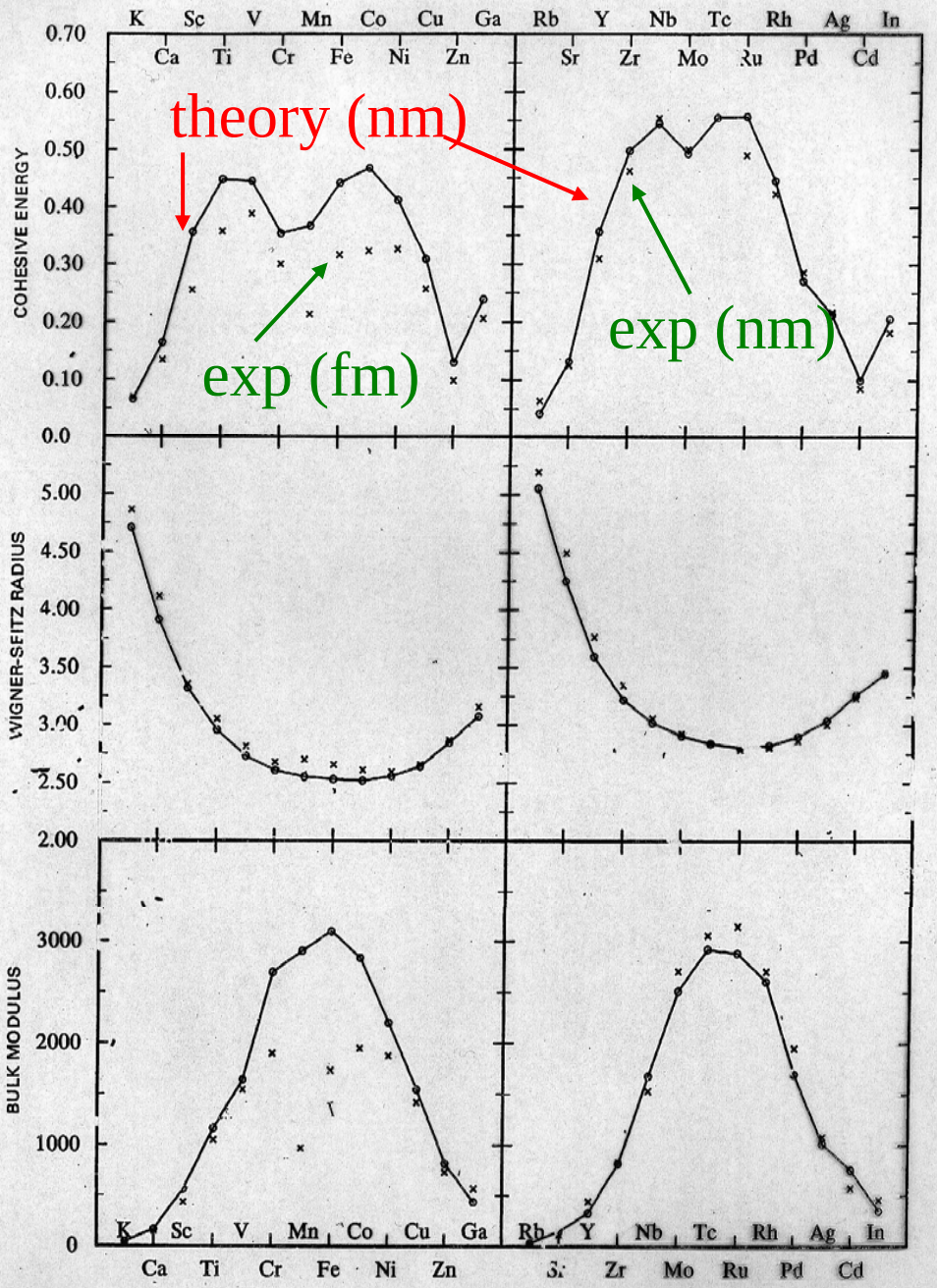

Figure 1.1 Cohesive properties. Top row- cohesive energy (Ry/atom). Middle row- Wigner-Seitz radius (a.u.). Bottom row- bulk modulus (Kbar). Measured values are indicated by crosses.

Transition metal

Ru

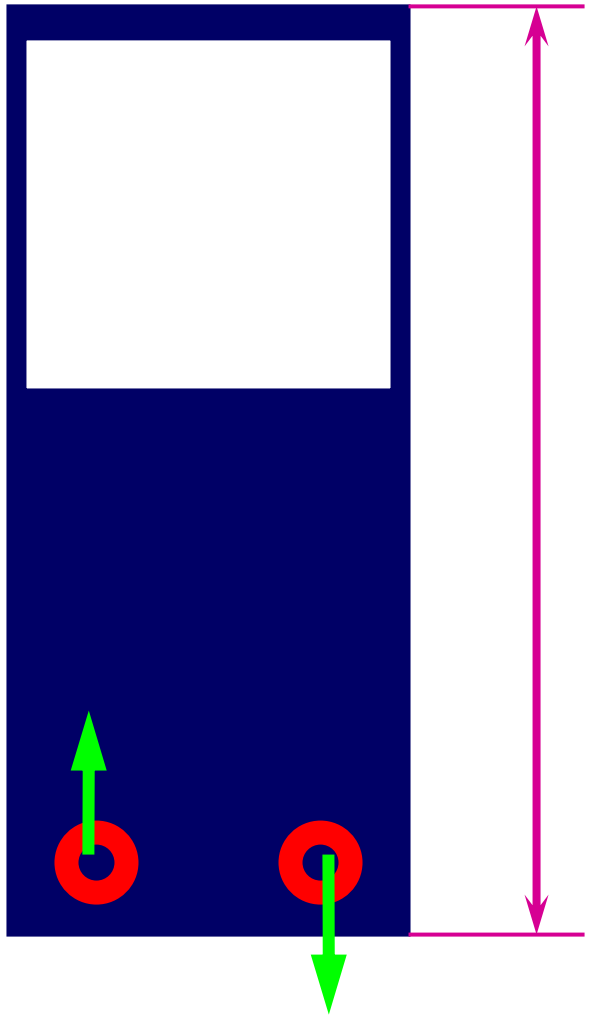

$$E_{BOND} = -\frac{1}{20} W N_d (10 - N_d)$$

Transition metal

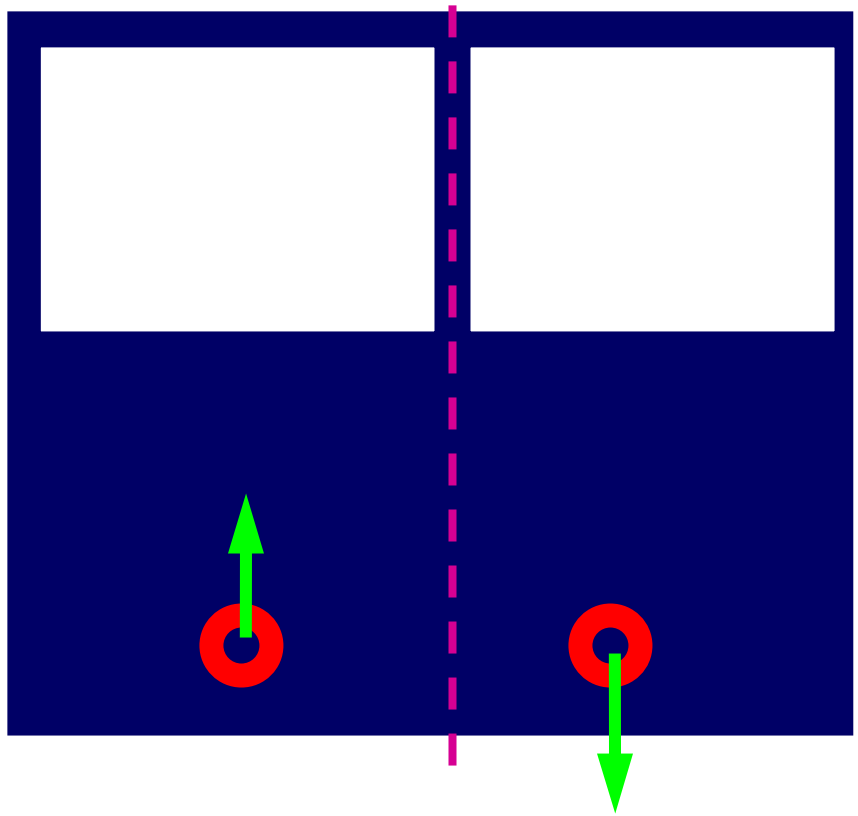

Fe

E_F

$$E_{BOND} = -\frac{1}{20} W N_d (10 - N_d)$$

$$E_{BOND} = \int_{\substack{spin\\up\\band}}^{E_F} (E - E_{valence}^{atom}) n(E) dE$$

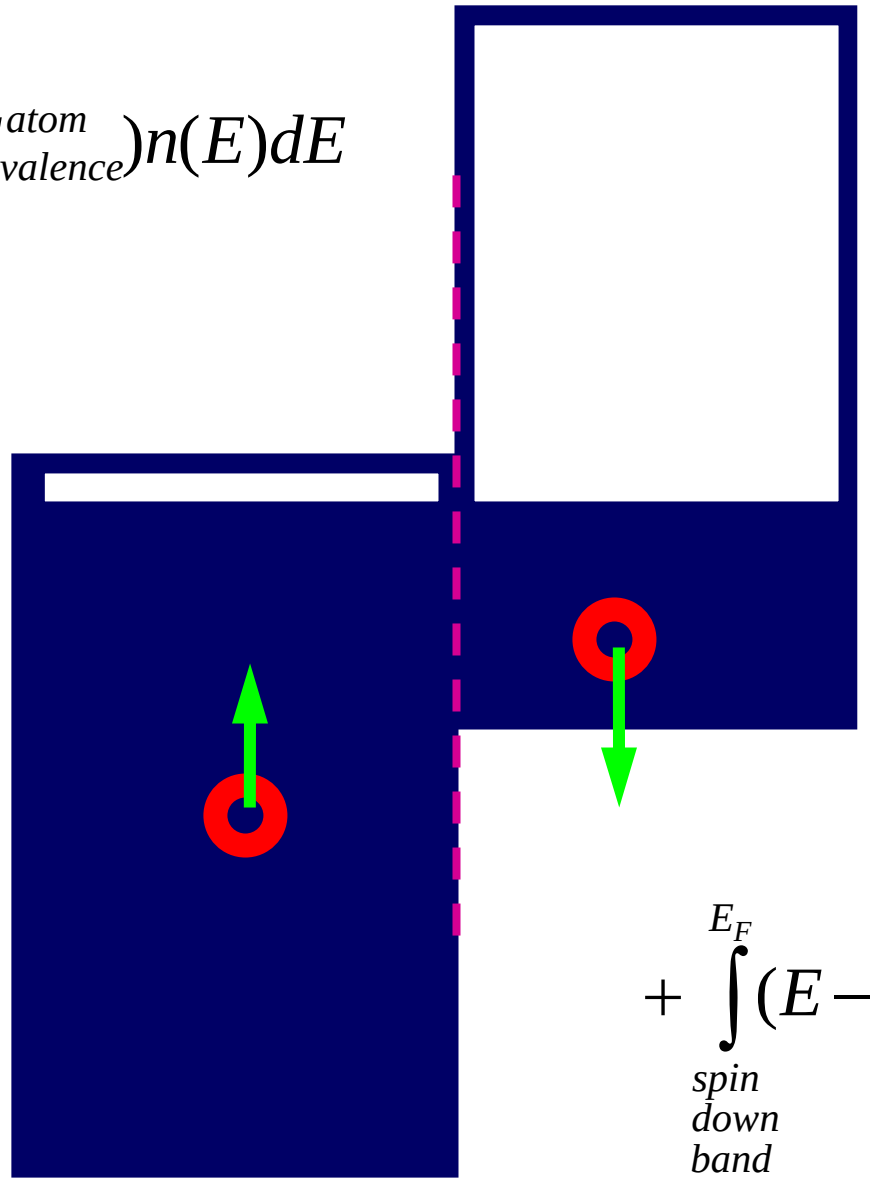

$$+ \int_{\substack{spin\\down\\band}}^{E_F} (E - E_{valence}^{atom}) n(E) dE$$

DIFFERENT PROPERTIES !!!

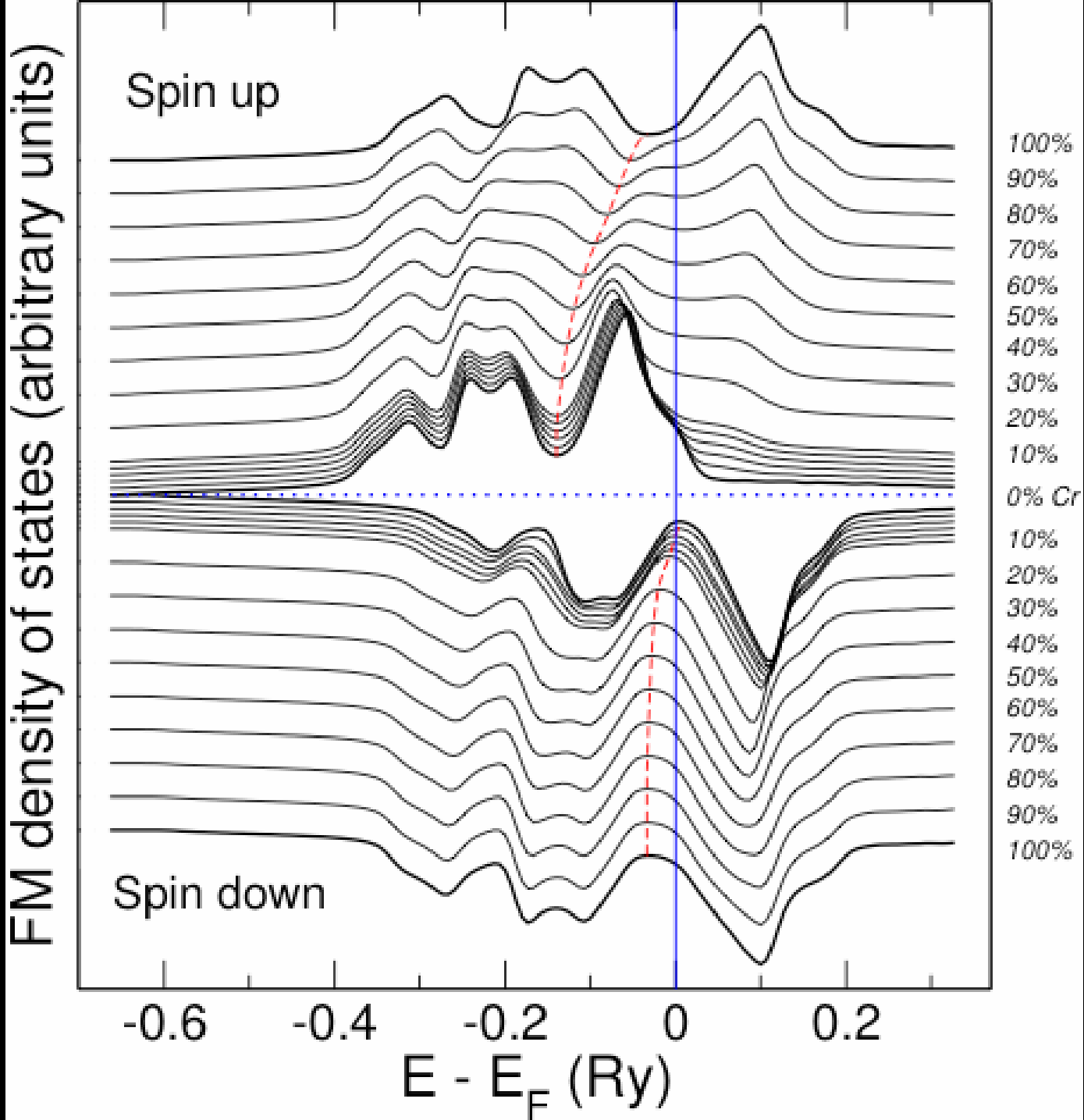
Spin up
Spin down
FM density of states (arbitrary units)
E - E_F (Ry)
-0.6
-0.4
-0.2
0
0.2
100%
90%
80%
70%
60%
50%
40%
30%
20%
10%
0% Cr
10%
20%
30%
40%
50%
60%
70%
80%
90%
100%

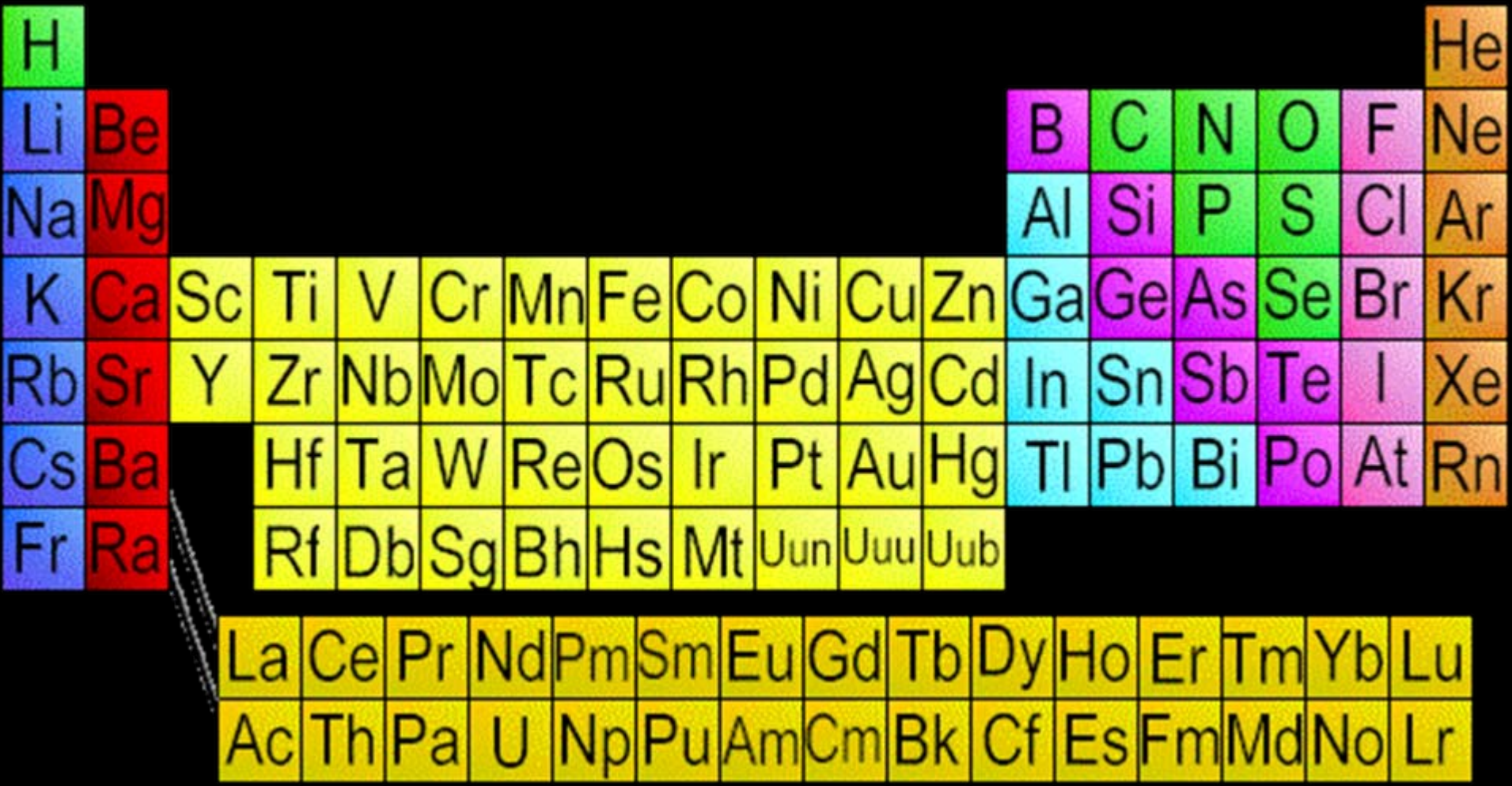
H
He
Li
Be
B
C
N
O
F
Ne
Na
Mg
Al
Si
P
S
Cl
Ar
K
Ca
Sc
Ti
V
Cr
Mn
Fe
Co
Ni
Cu
Zn
Ga
Ge
As
Se
Br
Kr
Rb
Sr
Y
Zr
Nb
Mo
Tc
Ru
Rh
Pd
Ag
Cd
In
Sn
Sb
Te
I
Xe
Cs
Ba
Hf
Ta
W
Re
Os
Ir
Pt
Au
Hg
Tl
Pb
Bi
Po
At
Rn
Fr
Ra
Rf
Db
Sg
Bh
Hs
Mt
Uun
Uuu
Uub
La
Ce
Pr
Nd
Pm
Sm
Eu
Gd
Tb
Dy
Ho
Er
Tm
Yb
Lu
Ac
Th
Pa
U
Np
Pu
Am
Cm
Bk
Cf
Es
Fm
Md
No
Lr

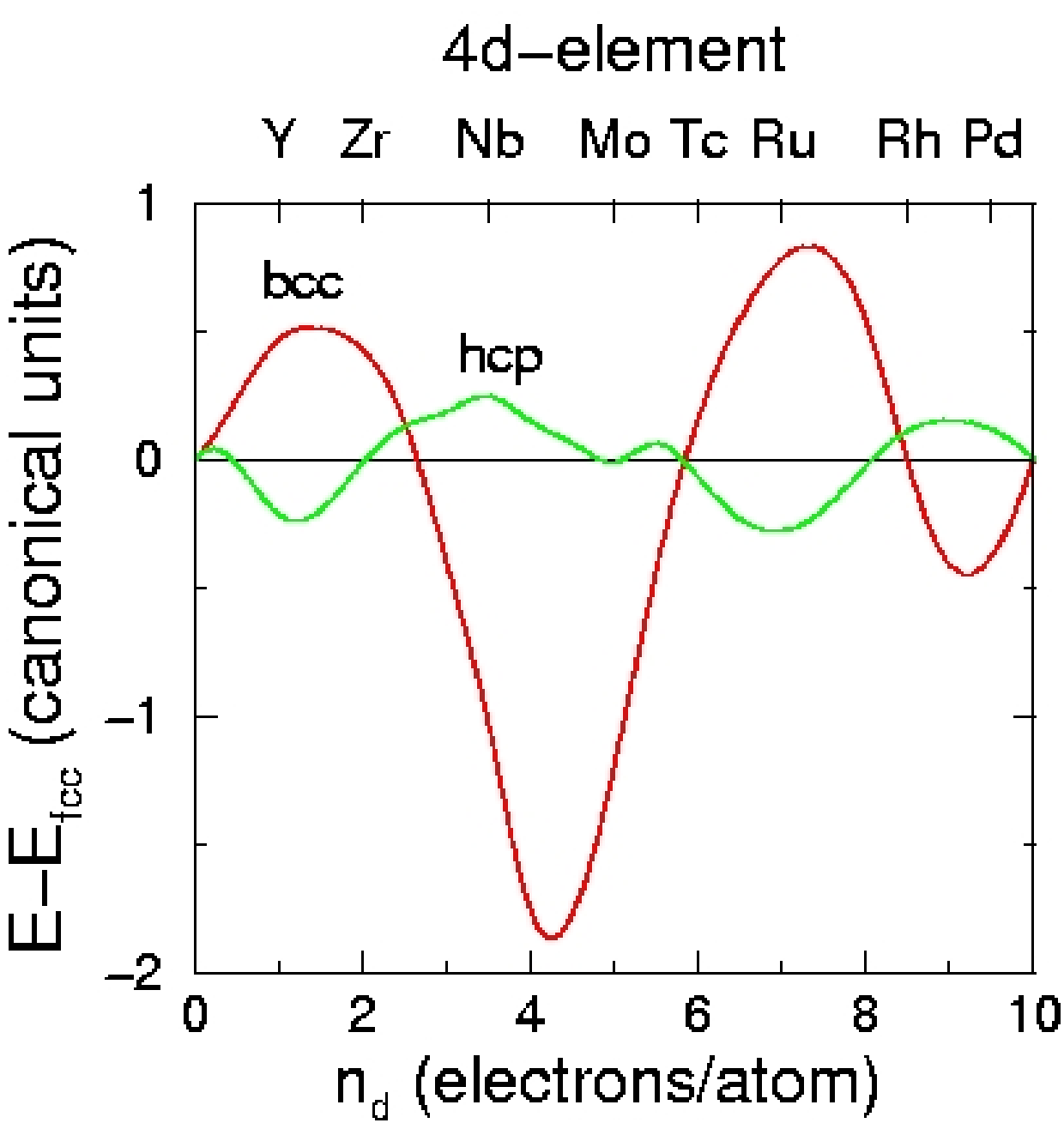
4d–element
Y Zr Nb Mo Tc Ru Rh Pd
bcc
hcp
1
0
–1
–2
0
2
4
6
8
10
E–E$_{fcc}$ (canonical units)
n$_d$ (electrons/atom)

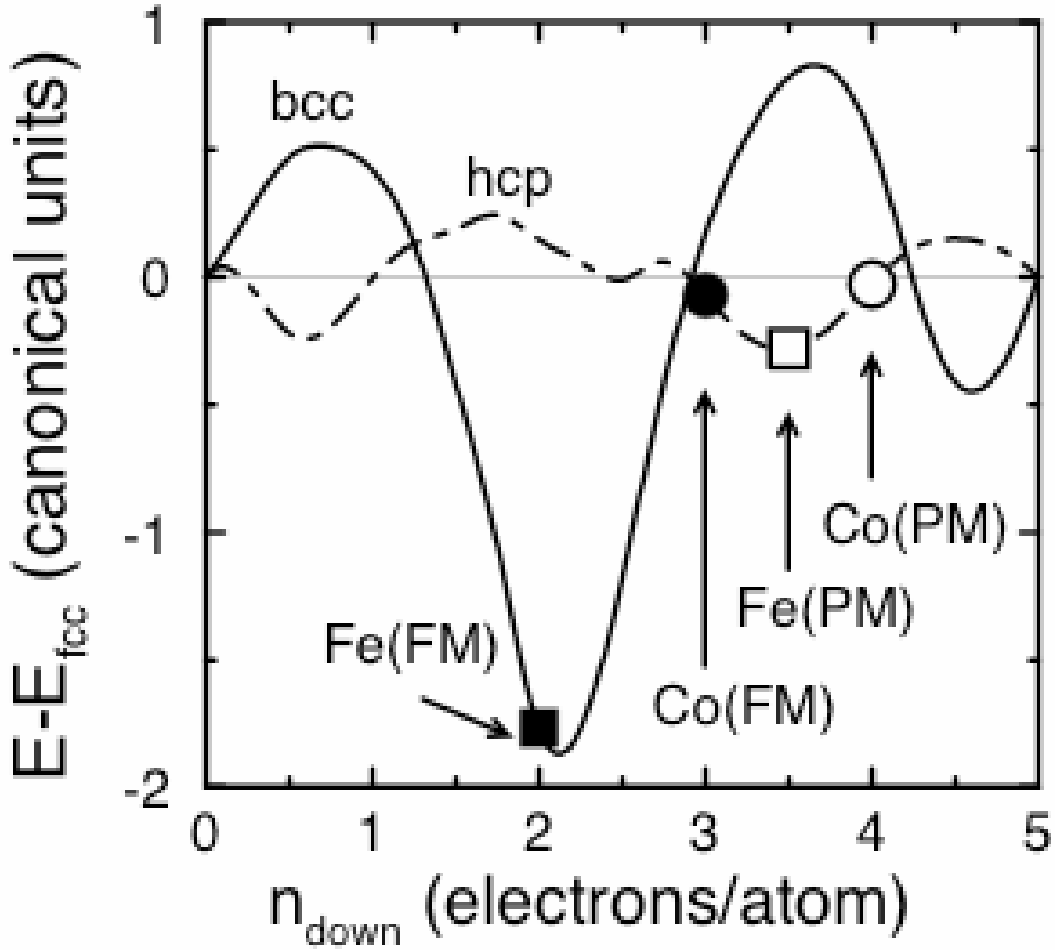
bcc
hcp
Fe(FM)
Co(FM)
Fe(PM)
Co(PM)
E-E$_{fcc}$ (canonical units)
n$_{down}$ (electrons/atom)
1
0
-1
-2
0
1
2
3
4
5

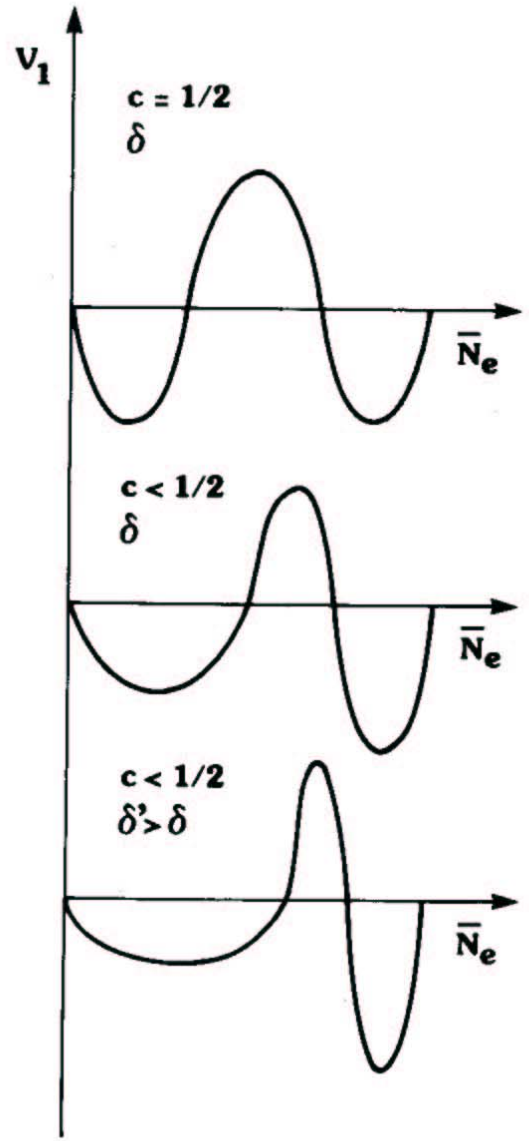

Fig. 7.5. Typical variations of $V_1(\bar{N}_e)$ for different values of c and of δ.

J. Phys. F: Met. Phys. 13 (1983) 2351–2358. Printed in Great Britain

Chemical SRO effects in ferromagnetic Fe alloys in relation to electronic band structure

M Hennion

Laboratoire Léon Brillouin, CEN Saclay, 91191 Gif-sur-Yvette Cédex, France

Received 3 May 1983

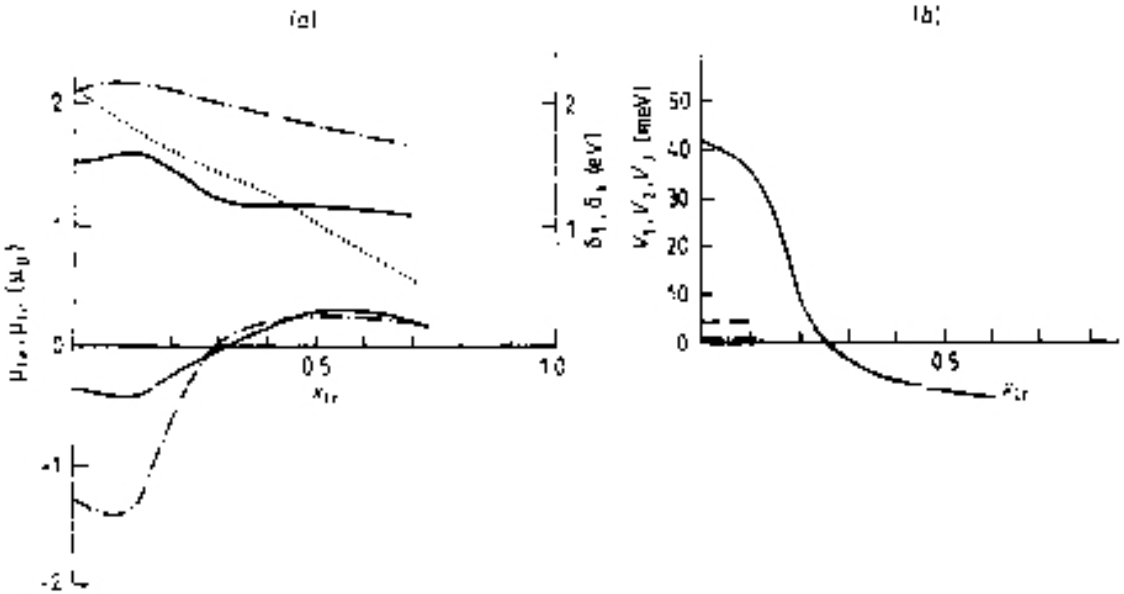

Figure 2. FeCr alloys. (*a*) Calculated curves of the partial $\mu_{Fe}(c)$ and $\mu_{Cr}(c)$ ($\cdot - \cdot -$) and total (- - -) magnetisations, and calculated curves of the energy disorder parameters δ_σ ($\sigma = \uparrow, \downarrow$) with chromium concentration (——). (*b*) Calculated variations of the pair potentials with Cr concentration: V_1(——), V_2(· · ·) and V_3(· - · -).

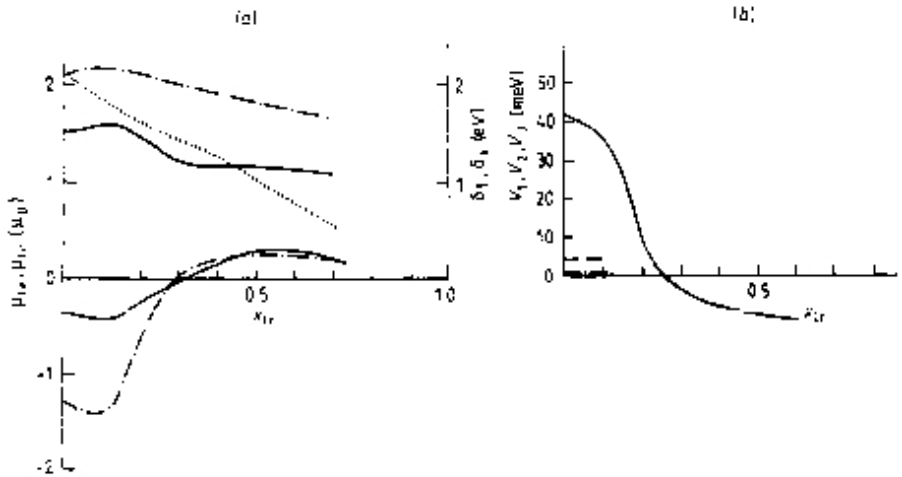

Figure 2. FeCr alloys. (*a*) Calculated curves of the partial $\mu_{Fe}(c)$ and $\mu_{Cr}(c)$ ($\cdot - \cdot - \cdot$) and total ($\cdots$) magnetisations, and calculated curves of the energy disorder parameters δ_σ ($\sigma = \uparrow, \downarrow$) with chromium concentration (——). (*b*) Calculated variations of the pair potentials with Cr concentration: V_1(——), V_2( ) and V_3($\cdot - \cdot - \cdot$).

NN pair potentials , mRy

Cr concentration, at.%

CONCLUSIONS :

- First-principles simulations can be carried out for real materials of technological importance.
- The results allow for the cautious optimism, and the choice of methodology should depend on the problem at hand.
- The mixing enthalpy for paramagnetic alloys is positive at all concentrations, in excellent agreement with experiment.
- On the contrary, ferromagnetic bcc Fe-Cr alloys are anomalously stable at low Cr concentrations. Therefore, magnetic effects must be taken into account in simulations.
- The stability of the ferromagnetic alloys is determined by the strong concentration dependence of interatomic interactions in this system, which therefore must be taken into account in simulations.